STOCHASTIC RESPONSE OF ISOLATED STRUCTURES UNDER EARTHQUAKE EXCITATIONS

by

CIBI JACOB M.

Department of Civil Engineering

Submitted in fulfillment of the requirement of the degree of

MASTER OF TECHNOLOGY

To the

Indian Institute of Technology Delhi

Hauz Khas, New Delhi - 110 016

May 2010

Certificate

This is to certify that the thesis titled **Stochastic Response of Isolated Structures under Earthquake Excitations**, submitted by **Cibi Jacob M**, to the department of Civil Engineering, Indian Institute of Technology Delhi, to fulfill the partial requirements for the award of the degree of **Master of Technology** in Structural Engineering, is a bonafide record of the research work done by him under our supervision.

The contents of this thesis, in full or in parts, have not been submitted to any other Institute or University for the award of any degree or diploma to the best of our knowledge.

Dr. Vasant Matsagar
Department of Civil Engineering,
Indian Institute of Technology, Delhi,
New Delhi, India.

Dr-Ing. Steffen Marburg
Institut für Festkörpermechanik,
Technische Universität Dresden,
Dresden, Germany.

This thesis is dedicated to my loving parents

Abstract

One of the emerging tools for protecting structures from the damaging effects of earthquakes is the use of isolation systems. Seismic isolation is achieved via inserting flexible isolator elements which lengthens the vibration period and increase energy dissipation. This study investigates the stochastic response of a base-isolated building considering the uncertainty in the characteristics of the earthquakes. For this purpose a probabilistic ground motion model, for generating artificial earthquakes is developed. The model is based upon a stochastic ground motion model which has separable temporal and spectral non-stationarities. A database of recorded earthquake ground motions is created. The parameters required by the stochastic ground motion model to depict a particular ground motion are found out for all the ground motions in the database. Probability distributions are created for all the parameters. Using Monte Carlo simulations the parameters required by the stochastic ground motion model to simulate ground motions are obtained from the distributions and ground motions. A bilinear model of the isolator described by its characteristic strength, post-yield stiffness and yield displacement is used and the stochastic response is calculated by using an ensemble of generated earthquakes. A parametric study is done for the various characteristics of the isolator. Reliability analysis is carried out on the base-isolated structure. It is found that base isolation is very effective for more than 99 percent of the earthquakes generated.

Keywords : Base Isolation, Stochastic Response, Ground Motion Model, Artificial Earthquakes, Bilinear Model, Reliability

Acknowledgements

I would like to express my deepest gratitude to my supervisors, Dr.-Ing. Steffen Marburg for the invaluable assistance, knowledge and encouragement that I have received during the entire duration of my thesis work in Germany and Dr. Vasant Matsagar for all the support and motivation that I have recieved from him during this thesis work and during my entire stay at IIT Delhi.

I express sincere gratitude to Dr. Kheirollah Sepahvand for his guidance in my project work. I would like to thank Prof T.K. Datta who introduced me to the concepts of Earthquake Engineering. I express sincere thanks to all the faculty members of the Department of Civil Engineering, Indian Institute of Technology Delhi for their guidance and valuable suggestions during my course work.

I would also like to express my gratitude towards Deutscher Akademischer Austausch Dienst (DAAD) for providing me this opportunity to do my thesis work at Technische Universität Dresden. I would like to thank Mr. Markus Rimmele, Mr. Victor Vincze, and Mrs. Eva Kallinich, for helping me throughout my stay in Dresden and making it an unforgettable experience. I also express thanks to my friends and well wishers for their underlying support shown during this project.

Finally, I would like to express sincere gratitude towards my parents, brother and sister for their sincere love and prayers and for always being there for me.

Cibi Jacob M.

2008CES2509

X

Contents

List of Figures

List of Tables

Chapter 1

Introduction

1.1 Base Isolation

Base isolation, also known as seismic or base isolation system, is a collection of structural elements which should substantially decouple a superstructure from its substructure resting on a shaking ground thus protecting a building or non-building structure's integrity.

Base isolation intends to decouple the structure from seismic ground motion, minimizing, simultaneously, the interstorey deformations and the floor accelerations by interposing elements of high axial and low horizontal stiffness between the structure and the foundation.

Base isolation is the most powerful tool of the earthquake engineering pertaining to the passive structural vibration control technologies. It is meant to enable a building or non-building structure to survive a potentially devastating seismic impact through a proper initial design or subsequent modifications. In some cases, application of base isolation can raise both a structure's seismic performance and its seismic sustainability considerably. Contrary to popular belief base isolation does not make a building earthquake proof.

Even though the concept of base isolation has been introduced from the beginning of the 19th century, it has been extensively studied and applied to engineering

practice only during the last 25 years. Although there are various systems, base isolation techniques follow two basic approaches.

1.1.1 Elastomeric systems

In this approach, the isolation system introduces a layer of low lateral stiffness between the structure and its foundation. Due to the introduction of this layer, the structure has a natural period that is longer than its fixed base natural period. This reduces the earthquake induced force in the structure, but the deformation is increased due to the deformation in the isolation system.

Figure 1.1: Photo of a bearing system with all the elements. Source: [1]

Figure 1.2: Photo showing deformed shape of a isolator. Source: [2]

The most commonly used systems of this type use short, cylindrical bearings with alternating layers of steel and hard rubber. Interposed between the base of the structure and the foundation, these laminated bearings are strong and stiff under vertical loads but very flexible under lateral forces. Since the natural damping of rubber is low, additional damping is usually provided by means of a mechanical damper. These can be lead plugs inside the bearing, steel coils or hydraulic dampers. These metallic dampers provide energy dissipation through yielding, thus non-linearity is introduced in the system.

Figure 1.1 and Figure 1.2 show the photos of a bearing system with all the elements and deformed shape of a laminated rubber bearing (LRB).

1.1.2 Sliding systems

This system uses rollers or sliders in between the base of the structure and the foundation. The shear force transmitted to the structure across the isolation interface is limited by keeping the coefficient of friction as low as practical. But the friction should be sufficiently high to sustain high wind forces and minor earthquakes, this reduces the isolation effect.

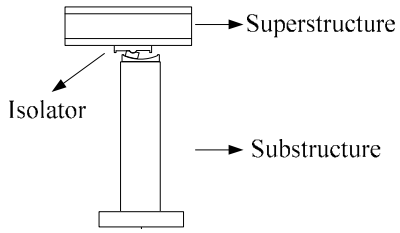

Figure 1.3: Sketch of a sliding system. Source: [3]

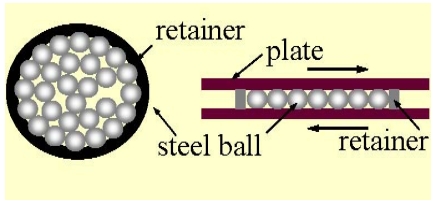

Figure 1.4: Sketch of a ball bearing. Source: [1]

In this type of isolation system, the sliding displacements are controlled by high tension springs or laminated rubber bearings, or by using concave dish of rollers. These mechanisms which provide a restoring force, otherwise unavailable in this system, help in bringing the structure back to its equilibrium. The dynamics of structures on this type of isolation system is highly complicated as the slip process is intrinsically non-linear.

Figure 1.3 and Figure 1.4 show the sketch of a sliding system with all the elements and a sliding type isolator

1.2 Stochastic Response

Generally, structural analysis is based on a deterministic concept. Observed variations in loading conditions, material properties, geometry, etc. are taken into account by either selecting extremely high or low or average values, respectively, for representing the parameters. Hence, by this, uncertainties inherent in almost every

analysis process are considered just intuitively. Observations and measurements of physical processes, however, clearly show their random characteristics.

Structural engineering design is filled with uncertainties, some of which are obvious and some of which many engineers may never have considered. Uncertainty can be separated into two categories: Aleatory, related to luck or chance, and epistemic, related to knowledge [4].

Statistical and probabilistic procedures provide a sound frame work for a rational treatment of analysis of these uncertainties. Moreover, there are various types of uncertainties. The entire spectrum of uncertainties is also not known. In reality, neither the true model nor the model parameters are deterministically known [5].

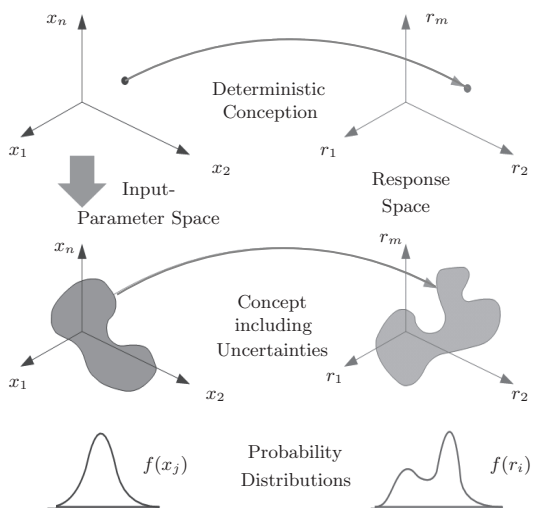

Figure 1.5: Deterministic concept versus stochastic concept. Source: [5]

In the deterministic concept, a single value is considered to be enough to represent a particular variable. It is in fact a great number of values, each associated with a certain probability of occurrence of a particular value, which is needed for a realistic description. Hence, the variables in their basic form may be described as random variables. The associated uncertainty are quantified by probability measures such as probability density functions.

Figure 1.5 explains the comparison between the deterministic concept and the stochastic concept.

1.2.1 Monte Carlo simulations

The evaluation of the stochastic response by the Monte Carlo simulation technique is a powerful method for highly non-linear systems as well as for systems where the input is modeled by large number of random variables [5].

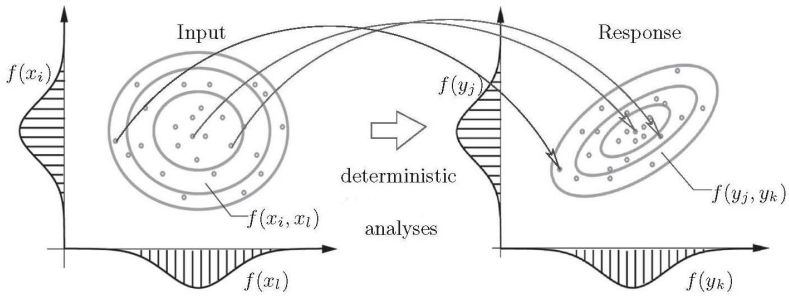

Figure 1.6: Stochastic analysis based on Monte Carlo simulation. Source: [5]

Figure 1.6 explains the basic principles of Monte Carlo sampling, where the laws of statistics are used to derive information on the variability of the response. By using a suitable random number generator, statistically independent samples of the input which follow the prescribed probability distributions of the uncertain parameters are generated. Let the system be described by the operator Q, so that a set of random input variables collected in a vector x is mapped to the output y,

$$Qx = y \tag{1.1}$$

In the simplest form of the Monte Carlo simulation technique, denoted as direct Monte Carlo simulation, for each generated sample of the input $x(i)$ the corresponding output $y(i)$ is calculated. Hence, the input distribution $f(x_1, x_2, ..., x_m)$ is represented according to statistical laws by a finite number of independent samples $x(i)_{i=1}^{n}$. Each vector $x(i)$ specifies for each uncertain parameter a deterministic discrete value and consequently defines deterministically the response which might be represented by the vector as follows

$$y^{(i)} = Qx^{(i)} \tag{1.2}$$

Hence, traditional deterministic analyses can be used to provide the mapping given by (1.2) between input and response.

In the simplest case, it might be justified to assume that all uncertainties are independent. Such an assumption is reasonable as long as this assumption does not contradict experience and physical properties.

1.3 Ground Motion Modeling

1.3.1 Characteristics of ground motion

Ground motion at a particular site due to earthquakes is influenced by source, travel path and local site conditions. The first relates to the size and source of the source mechanism of the earthquake. The second describes the path effects of the earth as the wave travels from the source to the site. The third describes the effects of the upper hundreds of meters of rocks and soil and the surface topography at the site.

It is well known that earthquake ground motions are nonstationary in both time and frequency domains. Temporal nonstationarity refers to the variation in the intensity of the ground motion in time. Spectral nonstationarity refers to the variation in the frequency content of the motion in time. Although temporal nonstationarity can be easily modeled by multiplying a stationary process by a time function, spectral nonstationarity is not so easy to model. However, both effects are important, particularly in the non-linear response analysis.

There are two types of uncertainties in ground motion prediction, epistemic and aleatory. Epistemic uncertainty is attributed to the incomplete knowledge and data about the physics of earthquake phenomenon. Aleatory uncertainty is due to the

fact that the future earthquakes are unpredictable. In principle, the former can be reduced by accumulating additional information but the latter cannot be reduced.

1.3.2 Need for ground motion modeling

The modeling, analysis and simulation of ground motion signals is of crucial importance in studying and improving the behaviour of structures under earthquake excitation and has thus attracted significant attention during the past several years.

The growing interest in performance-based earthquake engineering (PBEE) in recent years has further increased the need for stochastic modeling of ground motions. The PBEE analysis typically considers the entire spectrum of structural response, from linear to grossly non-linear and even collapse. For such an analysis, realistic characterization of the ground motion is essential. In the current PBEE practice, usually recorded ground motions are employed, which are then scaled to various levels of intensity. This approach suffers from scarcity of recorded ground motions for specified earthquake characteristics. Stochastic ground motion models provide an alternative for use in PBEE in lieu of or in conjunction with recorded ground motions.

1.4 Objectives and Scope

1.4.1 Objectives of the study

The objective of this study is to determine the stochastic response of an isolated building under earthquake excitations with an emphasis on the uncertainty in the earthquake loading. The research tasks to accomplish these objectives are the following:

1. Create a database of earthquakes and fit all the earthquakes to a stochastic ground motion model.

2. Determine the probability density function of all the parameters required to generate an artificial ground motion of required statistical characteristics.

3. Generate a large number of artificial ground motions. Perform stochastic response analysis and parametric studies.

4. Perform reliability analysis on the response of the base-isolated building.

1.4.2 Scope of the study

All the parameters of the structure and isolator such as mass, stiffness, damping, etc are considered to be deterministic. Only the uncertainty in the earthquakes is considered for finding the stochastic response.

The probabilistic model created for the earthquake loading is random in nature. There is no established connection to specific characteristics of the earthquake such as source, site conditions, etc.

1.5 Thesis Outline

The content of the dissertation is organized into the following chapters:

Chapter 2 provides a literature review on topics of interest for this study. Particular emphasis is given to the stochastic modeling of ground motion, base isolation, stochastic response and reliability analyses. A critical assessment of the current-state-of-the-art is presented.

Chapter 3 deals with the deterministic response of an isolated building structure under earthquake excitation. The modeling of the structure and isolator, governing equations of motion, solution procedure and an example are presented.

Chapter 4 explains the stochastic ground motion model selected for this study. Description of the various steps involved in generating a ground motion and identifying the parameters of the model is presented.

Chapter 5 describes about the database of the earthquakes. The identification of the parameters for the earthquakes in the database and their probability density function is described.

Chapter 6 presents a stochastic reponse analysis, parametric studies, study of the extreme response quantities and the reliability analysis of the response.

Chapter 7 presents a summary of the research, major conclusions drawn from this study, and recommendation for future research.

Chapter 2

Literature Review

2.1 Introduction

The introduction of seismic isolation as a practical tool has provided a rich source of literature on experimental and theoretical work, both in the dynamics of the isolated structural systems and in the mechanics of the isolators. Synthetic ground motions have been of interest in the field of earthquake engineering for many years. There is a lot of literature related to ground motion modeling. This chapter presents a summary of the previous studies that address the modeling of ground motions and various studies on base isolated structures.

2.2 Base Isolation

Reviews presented by Kelly [6], Buckle and Mayes [7], Ibrahim [8] and Jangid and Datta [9] summarize much of the literature on theoretical aspects of seismic isolation, testing programmes and isolation systems which have been used in buildings. These reviews describe the characteristics of the various implemented systems.

Matsagar and Jangid [10] studied the influence of isolator characteristics on the response of base-isolated structures by considering the isolator to have bilinear

hysteretic and equivalent linear elasticviscous behaviors. This study elaborates on the use of isolators with different model types and parameters.

Sharma and Jangid [11] studied the effect of high initial stiffness in the bilinear model of the isolator on the behaviour of base-isolated structures. They concluded that the floor accelerations and interstorey drifts are increasing significantly with the increase of the initial stiffness of the isolation system.

2.3 Ground Motion

There are two types of stochastic ground motion models: models that describe the random occurrence of fault ruptures at the source and propagation of the resulting seismic waves through the ground medium (source based models) and models that describe the ground motion for a specific site by fitting to a recorded motion with known earthquake and site characteristics (site based models). A review of source based models is presented by Zerva [12].

By using a site based stochastic model, one is able to generate artificial ground motions, which have statistical characteristics similar to those of the target ground motion. A large number of site based models have been proposed in the past. A review is presented by Shinozuka and Deodatis [13] and more recently by Conte and Peng [14].

Kiureghian and Crempien [15] proposed an evolutionary random process model for describing the earthquake ground motion. The model is composed of individually modulated component stationary processes, each component representing the energy in the process in a narrow band of frequencies. The model accounts for both temporal and spectral nonstationarity of the motion.

A probabilistic ground motion model was proposed by Papadimitriou [3] which is capable of capturing, with at most nine parameters, all those features of the ground acceleration history which have an important influence on the dynamic response of linear and non-linear structures, including the amplitude and frequency content

nonstationarities of the shaking. The model is based on bayesian probabilistic framework.

A fully nonstationary stochastic model for strong earthquake ground motion was developed by Rezaeian and Kiureghian [16]. The model employs filtering of a discretized white-noise process. Nonstationarity is achieved by modulating the intensity and varying the filter properties in time. The formulation has the important advantage of separating the temporal and spectral nonstationary characteristics of the process, thereby allowing flexibility and ease in modeling and parameter estimation.

2.4 Stochastic Response

Schüeller and Pradlwarter [17] presented a review on the various methods available for uncertainty analysis of complex structural systems. It is shown that advanced Monte Carlo simulation (MCS) procedures is the most versatile approach.

Er and Iu [18] studied the stochastic response of a rigid structure connected to a foundation with coulomb friction-type base isolation subjected to stationary Gaussian white noise type ground excitations. Analytical solutions were compared to MCS results.

Su and Ahmadi [19] did a study on the responses of a rigid structure with a frictional base isolation system subjected to random horizontal-vertical earthquake excitations. The ground accelerations were modelled by segments of stationary and nonstationary Gaussian white noise and filtered white noise processes. The differential equation governing the covariance matrix was solved and the results were compared with those obtained by a series of Monte-Carlo digital simulations and reasonable agreement was observed.

Analytical solutions for the stochastic response of practical sliding systems were proposed by Constantinou and Papageorgiou [20] and the results were verified by extensive Monte Carlo simulations.

Pradlwarter et al. [21] did a study on the application of controlled Monte Carlo simulation for studying the effect of a two dimensional hysteretic, friction based device assembled at particular locations throughout the structure.

In a study by Yeh and Wen [22], a stochastic model of ground excitation was proposed in which both intensity and frequency content are functions of time. Responses of single-mass inelastic systems and three-story space frames, with or without deterioration, under the nonstationary biaxial ground excitation were investigated via the equivalent linearization method and Monte Carlo simulations.

Alhan and Gavin [23] presented a paper on reliability analysis of a four storey structure representing a critical facility with an isolation floor, by including uncertainties such as isolation system characteristics, eccentricity in the superstructure, and ground motion characteristics. The Monte Carlo simulation technique was used to determine probability distributions and failure probabilities.

2.5 Summary

The bilinear behaviour of the isolator can be effectively used to model most of the isolation systems in practice. Stochastic ground motion models which consider both the spectral and temporal non stationarity effectively simulates recorded ground motions. There are few such models.

The uncertainty in the characteristics of the earthquake causes uncertainty in parameters of the ground motion model. A probabilistic model which takes into account the uncertainty in the parameters representing recorded earthquakes in the stochastic ground motion model has not been proposed. This necessitates the need for a probabilistic ground motion model which takes into account, the uncertainty of the characteristics of the earthquakes.

Previous studies [17] - [23] have demonstrated that Monte Carlo simulation is an effective method in obtaining stochastic response statistics. Studies show that the results have reasonable agreement to analytical solutions. Monte Carlo simulation is

a convenient and accurate method for calculating the probability of failure. Monte Carlo simulation can be used for analyses where analytical reliability methods such as First Order Reliability Methods (FORM), Second Order Reliability Methods (SORM) and Response Surface Methods (RSM) are difficult to use.

Chapter 3

Deterministic Response of an Isolated Building

3.1 Introduction

The procedure used to find the deterministic response of a base-isolated building under earthquake excitations is described in this chapter by considering a numerical example. The modeling involved, solution procedure and results are detailed below.

3.2 Modeling

Lumped mass modeling is done for the superstructure and the isolator. The effect of rotation in the structure and isolator is not taken into consideration.

3.2.1 Superstructure

The base-isolated building is modeled as a shear type structure mounted on isolation systems with one lateral degree-of-freedom at each floor. Figure 3.1 shows the idealized mathematical model of the five storey base-isolated building considered for the present study.

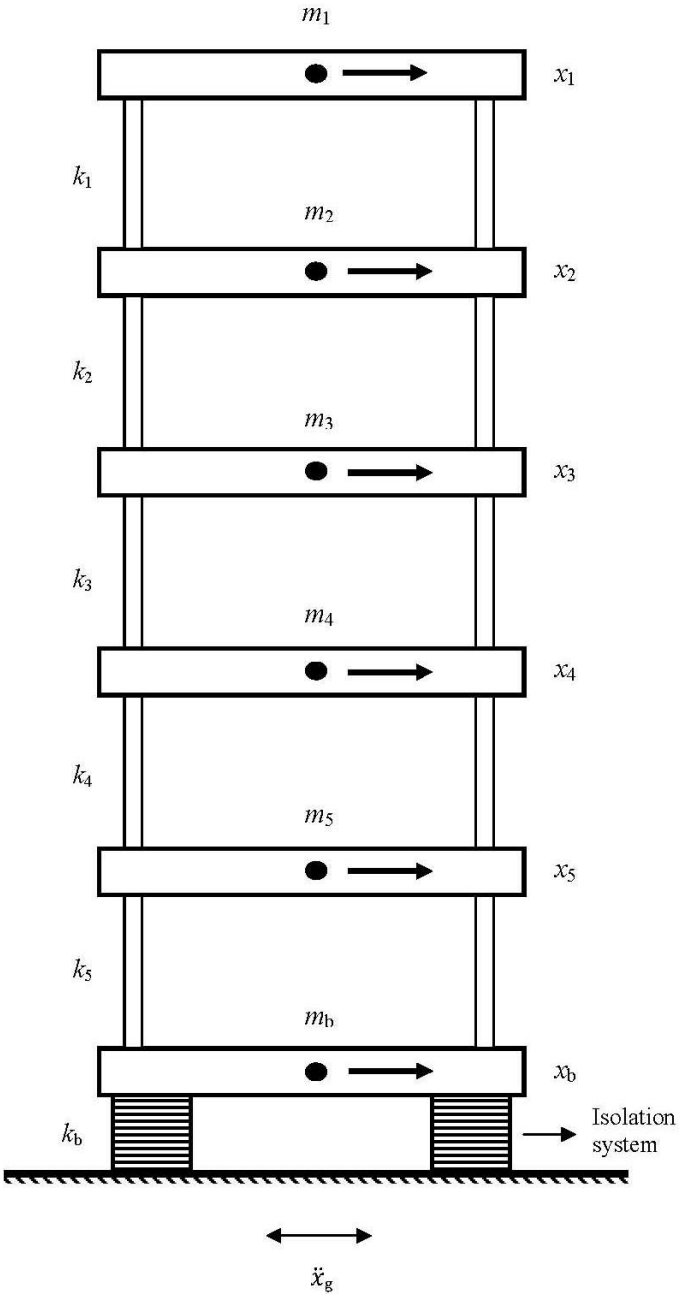

Figure 3.1: Mathematical model of the five storey base-isolated building

Following assumptions are made for the structural system under consideration:

1. The superstructure is assumed to remain within the elastic limit during the earthquake excitation.

2. The floors are assumed to be rigid in its own plane and the mass is lumped at

each floor level.

3. The columns are inextensible and weightless providing the lateral stiffness.

4. The system is subjected to a horizontal component of the earthquake ground motion in one direction.

5. The effect of soil structure interaction is neglected.

x_j is the relative floor displacement with respect to the isolator at the j^{th}floor, m_j is the floor mass at the jth th floor, k_j is the stiffness of the jth th floor, x_b is the displacement of the isolator and m_b is the mass of the isolator.

3.2.2 Isolators

For the present study, the force-deformation behaviour of the isolator is modeled as non-linear hysteretic represented by the bilinear model.The model is shown in Figure 3.2.

The non-linear force-deformation behaviour of the isolation system is modeled through the bilinear hysteresis loop characterized by three parameters namely:

1. Characteristic strength, Q

2. Post-yield stiffness, k_b and

3. Yield displacement, q.

The bilinear behaviour is selected because this model can be used for most of the isolation systems used in practice. The characteristic strength, Q is related to the yield strength of the lead core in the elastomeric bearings and friction coefficient of the sliding type isolation systems. The post-yield stiffness of the isolation system, k_b is generally designed in such a way to provide the specific value of the isolation period, T_b expressed as

$$T_b = 2\pi\sqrt{\frac{M}{k_b}} \tag{3.1}$$

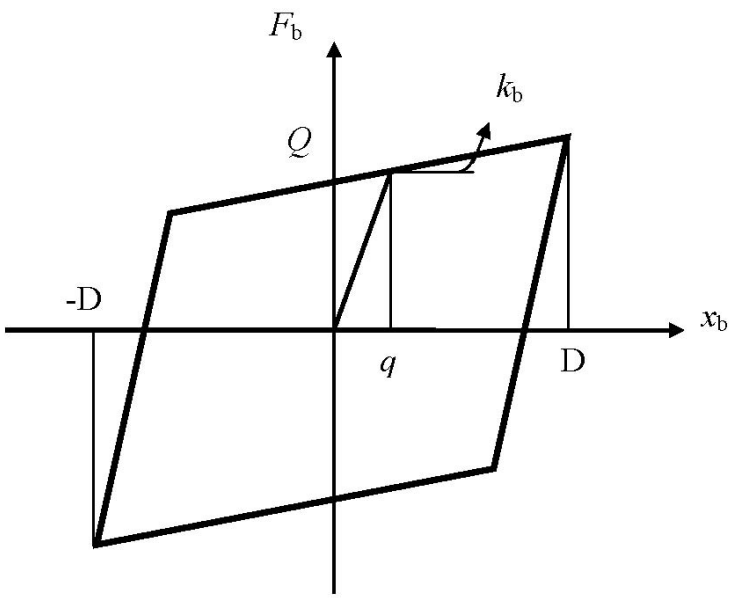

Figure 3.2: Mathematical model of the isolator

Where $M = (m_b + \sum_{j=1}^{5} m_j)$ is the total mass of the base-isolated structure. The characteristic strength, Q is mathematically related to the damping ratio, ζ_b by the following equation [24].

$$\zeta_b = \frac{4Q(D-q)}{2\pi k_b D^2} \tag{3.2}$$

Here D is the design displacement.

Thus, the bilinear hysteretic model of the base isolation system can be characterized by specifying the three parameters namely T_b, Q and q.

3.3 Governing Equations of Motion

The general equations of motion for the super structure-isolator model illustrated in Figure 3.1 can be expressed as

$$M\ddot{X}^{\text{Tot}}(t) + C\dot{X}(t) + KX(t) = 0 \tag{3.3}$$

Here $X = \{x_j\}^{\mathrm{T}}$ is the column vector of relative structural displacements with respect to the isolator and $X^{\mathrm{Tot}} = \left\{x_j^{\mathrm{Tot}}\right\}^{\mathrm{T}}$ is the column vector of total structural displacements. M is the mass matrix of structure, C is the damping matrix of structure and K is the stiffness matrix of structure.

$$x_j^{\mathrm{Tot}} = x_j + x_b + x_g \tag{3.4}$$

Where x_g is the displacement of the ground due to the earthquake. x_b is the displacement of the isolator.

Now for the five storey base isolated building the governing equations of motions are given by

$$M\ddot{X}(t) + C\dot{X}(t) + KX(t) = -\overline{M}\ddot{x}_g \tag{3.5}$$

where

$$M = \begin{bmatrix} m_1 & 0 & 0 & 0 & 0 & m_1 \\ 0 & m_2 & 0 & 0 & 0 & m_2 \\ 0 & 0 & m_3 & 0 & 0 & m_3 \\ 0 & 0 & 0 & m_4 & 0 & m_4 \\ 0 & 0 & 0 & 0 & m_5 & m_5 \\ 0 & 0 & 0 & 0 & 0 & m_b \end{bmatrix} \tag{3.6}$$

$$K = \begin{bmatrix} k_1 & -k_1 & 0 & 0 & 0 & 0 \\ -k_1 & k_1 + k_2 & -k_2 & 0 & 0 & 0 \\ 0 & -k_2 & k_2 + k_3 & -k_3 & 0 & 0 \\ 0 & 0 & -k_3 & k_3 + k_4 & -k_4 & 0 \\ 0 & 0 & 0 & -k_4 & k_4 + k_5 & -k_5 \\ 0 & 0 & 0 & 0 & -k_5 & k_5 + k_b \end{bmatrix} \tag{3.7}$$

$$\overline{M} = \{m_1, m_2, m_3, m_4, m_5, m_b\}^{\mathrm{T}} \tag{3.8}$$

$$X = \{x_1, x_2, x_3, x_4, x_5, x_b\}^{\mathrm{T}} \tag{3.9}$$

The damping matrix of the superstructure, C is not known explicitly. It is constructed by assuming the modal damping ratio for superstructure, which is kept constant.

3.4 Solution Procedure

Classical modal superposition technique cannot be employed in the solution of equations of motion here because (i) there is a difference in the damping in isolation system compared to the damping in the superstructure and (ii) the force-deformation behavior for the isolation systems considered is non-linear. Therefore, the equations of motion are solved numerically using Newmark's method of step-by-step integration [25]; adopting linear variation of acceleration over a small time interval of Δt.

The response quantities of interest such as acceleration, velocity and displacement at any degree of freedom, force in the isolator are calculated at each time interval. The force in the isolator is calculated by using Wen's model [26] from the

non-linear force-deformation diagram. A FORTRAN program is developed for this purpose.

3.5 Numerical Example

To find the deterministic response of the isolated structure, a recorded earthquake accelerogram is considered. The response is calculated and the results are plotted. The response quantities of interest are the top floor absolute acceleration and relative isolator displacement. The above response quantities are chosen because the floor accelerations developed in the superstructure are proportional to the forces exerted due to earthquake ground motion and the bearing displacements are important for the design of isolation systems.

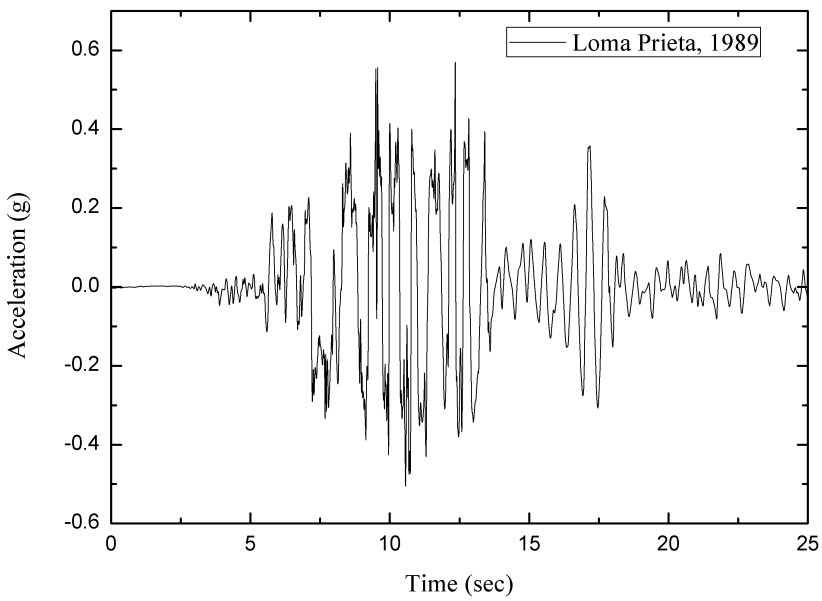

Figure 3.3: Time history of the Loma Prieta, 1989 earthquake

Table 3.1: Summary of parameters of the superstructure

S. No.	Parameter	Value
1	Ratio of floor mass	1:1:1:1:1
2	Ratio of floor stiffness	2:3:4:5:6
3	Damping Ratio of each floor	0.02
4	Time period of the superstructure, T_s	0.5 sec

3.5.1 Ground Motion

The earthquake motion selected for the study is N00E component of 1989 Loma Prieta earthquake recorded at Los Gatos Presentation Center. The peak ground acceleration (PGA) of Loma Prieta earthquake is 0.57g. The time history of the earthquake ground motion selected is shown in Figure 3.3

3.5.2 Structure and Isolator Parameters

The various parameters of the superstructure and the isolator considered for this example is described in this section. The summary of parameters considered for the super structure is given in Table 3.1 and the summary of parameters considered for the isolator is given in Table 3.2. The floor mass of each floor of the structure is considered to be equal. The stiffness is considered is such a way that the top floor are less stiffer than the bottom floors. The stiffness increases proportionally from top to bottom. Approximate time period of a five storey building is considered. The damping ratio of the superstructure is taken as 0.02 and kept constant for all modes of vibration. The inter-story stiffness of the superstructure is adjusted such that a specified fundamental time period of the superstructure, T_s is achieved. The mass of the isolator is considered to be equal to that of a floor.

Table 3.2: Summary of parameters of the isolator

S. No.	Parameter	Value
1	Ratio of floor mass to isolator mass	1:1
2	Damping Ratio of the isolator, ζ_b	0.1
3	Time period of the isolator, T_b	2.0 sec
4	Design Displacement, D	53.61 cm
5	Yield displacement, q	2.5 cm

3.5.3 Response Quantities

The response of the structure under the excitation of the recorded ground motion of Loma Prieta, 1989 earthquake is plotted. The time variation of the top floor acceleration of the base-isolated structure and the structure with a fixed base is shown in Figure 3.4. The effectiveness of base isolation is evident as we can see a significant reduction in the quantity of the peak top floor acceleration. The peak top floor acceleration of the fixed base structure is 2.92g and that of the base-isolated structure is 0.66g. The time variation of the displacement in the base-isolator is shown in Figure 3.5. The peak isolator displacement is 42.57 cm.

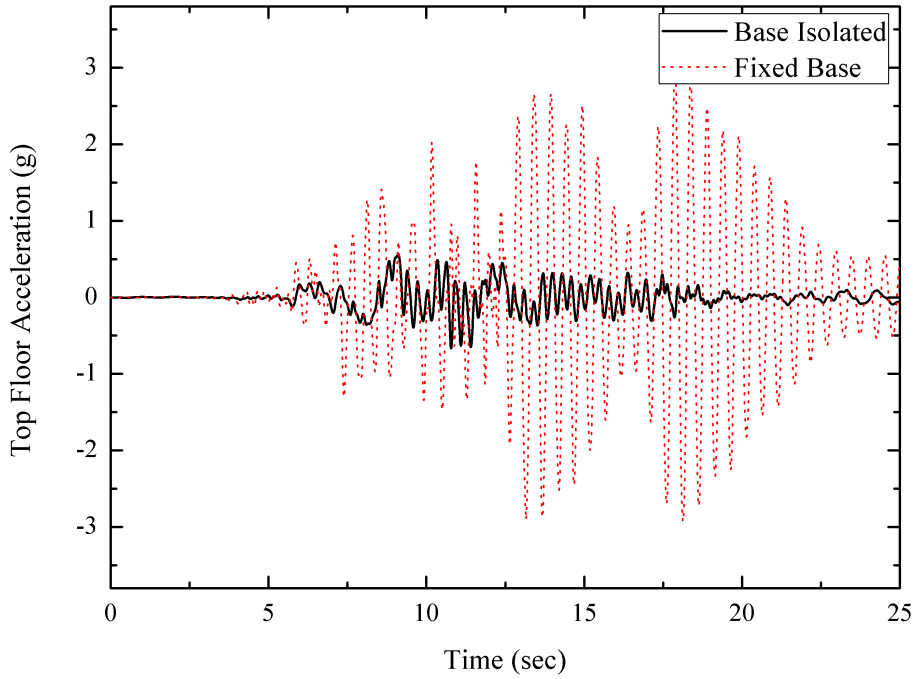

Figure 3.4: Time variation of top floor acceleration

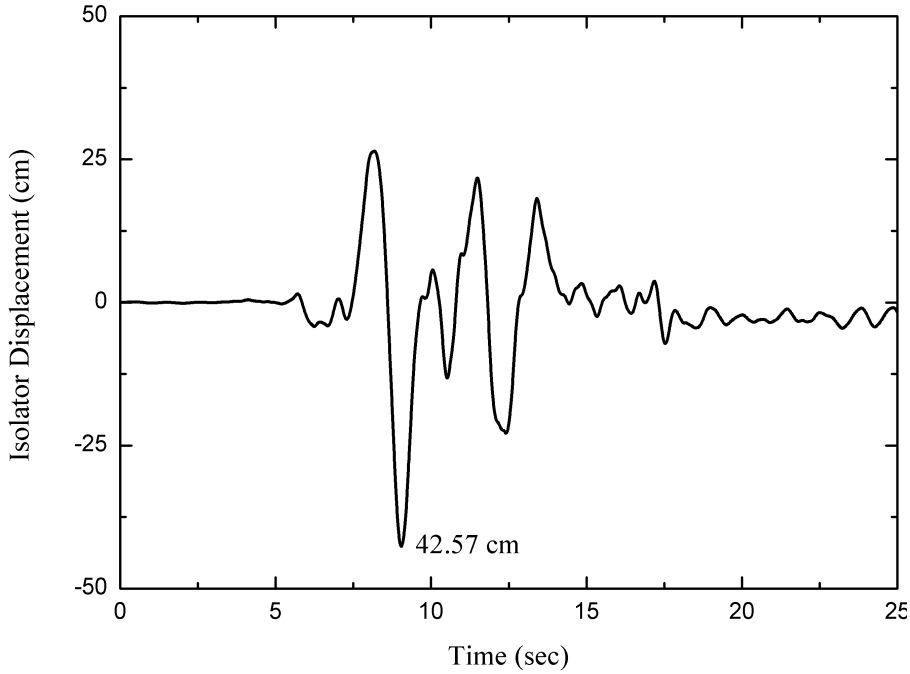

Figure 3.5: Time variation of isolator displacement

Chapter 4

Stochastic Ground Motion Model

4.1 Introduction

The stochastic ground motion model used in the present study is described in detail in this chapter. This fully nonstationary stochastic ground motion model uses filtering of a discretized white-noise process. Nonstationarity is achieved by modulating the intensity and varying the filter properties in time. The various steps involved in this model is described in this chapter.

4.2 Advantages of the Model

The stochastic ground motion model selected considers both the temporal and spectral nonstationarities. The selected model has the following advantages:

1. The model has a small number of parameters, which control the temporal and spectral nonstationary characteristics of the simulated ground motion and can be easily identified by matching with similar characteristics of the target accelerogram.

2. The temporal and spectral nonstationary characteristics are completely separable, facilitating identification and interpretation of the parameters.

3. There is no need for sophisticated processing of the target accelerogram, such as the Fourier analysis or estimation of evolutionary power spectral density.

4. The filter model provides physical insight and its parameters can be related to the characteristics of the earthquake and site considered.

5. Simulation of sample functions is simple and requires little more than generation of standard normal random variables.

4.3 Modulated Filtered White Noise Process

The modulated filtered Gaussian white noise process is obtained by time modulating the stationary response of a linear filter subjected to a Gaussian white noise excitation. Let the linear filter be defined by its impulse response function (IRF) $h(t, \theta)$, where θ denotes a set of parameters used to shape the filter response. Specifically, θ may include the natural frequency and damping of the filter, which control the predominant frequency and bandwidth of the process. We assume that the filter is causal so that $h(t, \theta) = 0$ for $t < 0$, and that it is stable, so that $\int_{-\infty}^{\infty} h(t, \theta)dt < \infty$ which also implies $\lim_{t\to\infty} h(t) = 0$. We also assume that $h(t, \theta)$ is at least once differentiable. This requires $h(t, \theta)$ to start from a zero value at $t = 0$ and not have any discontinuities.

The modulated filtered Gaussian white noise process can be expressed in the form [16]

$$x(t) = q(t) \left[\frac{1}{\sigma_h} \int_{-\infty}^{t} h(t - \tau, \theta)\omega(\tau)d\tau \right] \tag{4.1}$$

where $q(t)$ is the deterministic, non-negative modulating function, $\omega(t)$ denotes the Gaussian white noise process, τ is the time of application of the pulse and σ_h is the standard deviation of the filtered white noise process represented by the integral inside the square brackets.

Since the response of a stable filter to a white noise excitation becomes stationary after sufficient time, and since the white noise process is assumed to have started in the infinite past (the lower limit of the integral is $-\infty$), the filter response at any finite time point is stationary and, therefore, σ_h is a constant. One can easily show that

$$\sigma_h^2 = 2\pi S \left[\int_{-\infty}^{t} h^2(t-\tau,\theta) d\tau \right] \tag{4.2}$$

where S is the intensity of the white noise process.

The modulated filtered white noise process defined by (4.1) lacks spectral nonstationarity.

4.4 Fully Nonstationary Filtered White Noise Process

To achieve spectral nonstationarity with the filtered white-noise process the filter parameters are made to vary with time. Generalizing the form in (4.1), we define the fully nonstationary filtered white-noise process as

$$x(t) = q(t) \left[\frac{1}{\sigma_h(t)} \int_{-\infty}^{t} h[t-\tau,\theta(\tau)]\omega(\tau) d\tau \right] \tag{4.3}$$

where the parameters θ of the filter are now made dependent on the time of application of the load increment.

Naturally, the response of such a filter may not reach a stationary state. Therefore, the standard deviation $\sigma_h(t)$ of the process defined by the integral in (4.3) in general is a function of time. One can easily show that

$$\sigma_h^2 = 2\pi S \left[\int_{-\infty}^{t} h^2[t-\tau,\theta(\tau)] d\tau \right] \tag{4.4}$$

The modulating function $q(t)$ used to model ground motions usually starts from a zero value and gradually increases with time. Furthermore, the damping value of the filter used to model ground motions is usually large so that the IRF $h[t-\tau, \theta(\tau)]$ quickly diminishes with increasing $t - \tau$. Under these conditions, the lower limit of the integral in (4.3) and (4.4), which is $-\infty$, can be replaced with zero (or a finite negative value) without much loss of accuracy. This replacement offers computational convenience in the discretization of the process.

4.5 Discretization of the Nonstationary Process

In order to digitally simulate a stochastic process, discretization is necessary. Discretization is done in the time domain. The duration of the ground motion is discretized into a sequence of equally spaced time points $t_i = i \times \Delta t$ for $i = 0, 1, \ldots n$ where Δt is a small time step. At a time t, $0 < t < t_n$, letting $\left|\frac{t}{\Delta t}\right| = k$, where $0 \leq k \leq n$, the process in (4.3) can be expressed as

$$x(t) = q(t)\left[\frac{1}{\sigma_h(t)}\sum_{i=1}^{k}\int_{t_{i-1}}^{t_i} h[t-\tau, \theta(\tau)]\omega(\tau)\mathrm{d}\tau + \frac{1}{\sigma_h(t)}\int_{t_k}^{t} h[t-\tau, \theta(\tau)]\omega(\tau)\mathrm{d}\tau\right] \tag{4.5}$$

Assuming $h[t-\tau, \theta(\tau)]$ remains essentially constant during each small time interval $t_{i-1} \leq t \leq t_i$ and neglecting the last term, which is an integral over a fraction of the small time step, we get

$$\hat{x}(t) = q(t)\left[\frac{1}{\hat{\sigma}_h(t)}\sum_{i=1}^{k} h[t-t_i, \theta(t_i)]\int_{t_{i-1}}^{t_i}\omega(\tau)\mathrm{d}\tau\right] \tag{4.6}$$

$$\hat{x}(t) = q(t)\left[\frac{1}{\hat{\sigma}_h(t)}\sum_{i=1}^{k} h[t-t_i, \theta(t_i)]W_i\right],\ t_k \leq t < t_{k+1} \tag{4.7}$$

where

$$W_i = \int_{t_{i-1}}^{t_i} \omega(\tau)\mathrm{d}\tau \tag{4.8}$$

W_i for all i are statistically independent and identically distributed Gaussian random variables having zero mean and variance $2\pi S\Delta t$. Introducing the standard normal random variables $u_i = \frac{W_i}{\sqrt{2\pi S\Delta t}}$, (4.7) can be expressed as

$$\hat{x}(t) = q(t)\left[\frac{\sqrt{2\pi S\Delta t}}{\hat{\sigma}_h(t)}\sum_{i=1}^{k} h[t-t_i,\theta(t_i)]u_i\right],\ t_k \le t < t_{k+1} \tag{4.9}$$

We have superposed hats on two terms in the above expression. The one on $\hat{x}(t)$ is to highlight the fact that expressions (4.7) and (4.9) are for the discretized process and employ the approximations involved in going from (4.5) to (4.7). The hat on $\hat{\sigma}_h(t)$ is used to signify that this function is the standard deviation of the discretized process represented by the sum inside the square brackets in (4.7), so that the process inside the square brackets in (4.9) is properly normalized. Since W_i in (4.7) are statistically independent random variables, one has

$$\hat{\sigma}_h^2(t) = 2\pi S\Delta t\sum_{i=1}^{k} h^2[t-t_i,\theta(t_i)],\ t_k \le t < t_{k+1} \tag{4.10}$$

This equation is the discretized form of (4.4).

The representation in (4.9) has the simple form as follows

$$\hat{x}(t) = q(t)\sum_{i=1}^{k} s_i(t)\,u_i,\ t_k \le t < t_{k+1} \tag{4.11}$$

where

$$s_i(t) = \frac{\sqrt{2\pi S\Delta t}}{\hat{\sigma}_h(t)}\,h[t-t_i,\theta(t_i)] \tag{4.12}$$

$$s_i(t) = \frac{h[t - t_i, \theta(t_i)]}{\sum_{j=1}^{k} h^2[t - t_j, \theta(t_j)]},\ t_k \leq t < t_{k+1},\ 0 < i \leq k \tag{4.13}$$

4.6 Characterization of the Ground Motion Process

The intensity of a zero mean, Gaussian ground motion process which is characterized by its time varying standard deviation is defined by the modulating function $q(t)$. The frequency content may be characterized in terms of a predominant frequency and a measure of the bandwidth of the process, as they evolve in time. These properties of the process are influenced by the selection of the filter, i.e. the form of the IRF $h[t - \tau, \theta(\tau)]$, and its time-varying parameters $\theta(\tau)$.

As a surrogate for the predominant frequency of the process, here the mean zero-level up-crossing rate, $\nu(0^+, t)$, i.e. the mean number of times per unit time that the process crosses the level zero from below is used. Since the scaling of a process does not affect its zero-level crossings, $\nu(0^+, t)$ for the process in (4.11) is identical to that for the process

$$y(t) = \sum_{i=1}^{k} s_i(t)\, u_i,\ t_k \leq t < t_{k+1} \tag{4.14}$$

It is known that for such a process

$$\nu(0^+, t) = \frac{\sqrt{1 - \rho_{y\dot{y}}^2(t)}}{2\pi}\, \frac{\sigma_{\dot{y}}(t)}{\sigma_y(t)} \tag{4.15}$$

where $\sigma_y(t)$, $\sigma_{\dot{y}}(t)$ and $\rho_{y\dot{y}}^2(t)$ are the standard deviations and cross-correlation coefficient of $y(t)$ and its time derivative, $\dot{y}(t) = \frac{\mathrm{d}y(t)}{\mathrm{d}t}$ at time t. For the process in

(4.15), these are given by

$$\sigma_y^2(t) = \sum_{i=1}^{k} s_i^2(t) = 1,\ t_k \leq t < t_{k+1} \tag{4.16}$$

$$\sigma_{\dot{y}}^2(t) = \sum_{i=1}^{k} \dot{s}_i^2(t),\ t_k \leq t < t_{k+1} \tag{4.17}$$

$$\rho_{y\dot{y}}(t) = \frac{1}{\sigma_y(t)\sigma_{\dot{y}}(t)} \sum_{i=1}^{k} s_i(t)\dot{s}_i(t),\ t_k \leq t < t_{k+1} \tag{4.18}$$

where $\dot{s}_i(t) = \frac{\mathrm{d}s_i(t)}{\mathrm{d}t}$. Using (4.13) and $h_i(t) = h[t - t_i, \theta(t_i)]$, it is shown that

$$\dot{s}_i(t) = \left[\dot{h}_i(t) - \frac{\sum_{j=1}^{k} h_j(t)\dot{h}_j(t)}{\sum_{j=1}^{k} h_j^2(t)} h_i(t)\right] \frac{1}{\sqrt{\sum_{j=1}^{k} h_j^2(t)}},\ t_k \leq t < t_{k+1},\ 0 < i \leq k \tag{4.19}$$

For any differentiable IRF and filter parameter functions, the mean zero-level up-crossing rate of the process can be computed from (4.15) by use of the relations in (4.16) to (4.19). Naturally, the fundamental frequency of the filter will have a dominant influence on the predominant frequency of the resulting process.

4.7 Parameterization of the Model

A modified version of the Housner and Jennings model [27] as stated below is used as the modulating function.

$$q(t) = \begin{cases} 0 & t \leq T_0 \\ \sigma_{max} \left(\frac{t-T_0}{T_1-T_0}\right)^2 & T_0 < t \leq T_1 \\ \sigma_{max} & T_1 \leq t \leq T_2 \\ \sigma_{max}\ e^{[-\alpha(t-T_2)^\beta]} & T_2 \leq t \end{cases} \tag{4.20}$$

This model has six parameters T_0, T_1, T_2, σ_{max}, α and β which obey the conditions $T_0 < T_1 < T_2$, $0 < \sigma_{max}$, $0 < \alpha$ and $0 < \beta$. T_0 denotes the start time of the process, T_1 and T_2 denote the start and end times of the strong-motion phase with root mean square (RMS) acceleration σ_{max} and α and β are parameters that shape the decaying end of the modulating function.

Any damped single- or multidegree-of-freedom linear system that has differentiable response can be selected as the filter, here

$$h[t-\tau, \theta(\tau)] = \begin{cases} \frac{\omega_f(\tau)}{\sqrt{1-\zeta_f^2(\tau)}}\, e^{[-\zeta_f(\tau)\omega_f(\tau)(t-\tau)]} \sin\left[\omega_f(\tau)\sqrt{1-\zeta_f^2(\tau)}(t-\tau)\right] & \tau \leq t \\ 0 & \text{otherwise} \end{cases} \tag{4.21}$$

which represents the pseudo-acceleration response of a single-degree-of-freedom linear oscillator subjected to a unit impulse, in which τ denotes the time of application of the pulse. $\theta(\tau) = [\omega_f(\tau), \zeta_f(\tau)]$ is the set of parameters of the filter with $\omega_f(\tau)$ denoting the natural frequency and $\zeta_f(\tau)$ denoting the damping ratio, both dependent on the time of application of the pulse. $\omega_f(\tau)$ influence the predominant frequency of the resulting process, whereas $\zeta_f(\tau)$ influence its bandwidth. The predominant frequency of an earthquake ground motion tends to decay with time. Therefore,

$$\omega_f(\tau) = \omega_0 - (\omega_0 - \omega_n)\frac{\tau}{t_n} \tag{4.22}$$

in which t_n is the total duration of the ground motion, ω_0 is the filter frequency at time $t_0 = 0$ and ω_n is the frequency at time t_n. For a typical ground motion, $\omega_n < \omega_0$. Thus, the two parameters ω_0 and ω_n describe the time-varying frequency content of the ground motion.

Further analysis has shown that the linear form in (4.22) adequately characterizes the frequency variation of most recorded ground motions. The filter damping ζ_f can be considered a constant.

With the above parameterization, the stochastic ground motion model is completely defined by specifying the forms of the modulating and IRF functions, and the parameters that define them. Specifically, the six parameters (T_0, T_1, T_2, σ_{max}, α and β) define the modulating function in (4.20) and the three parameters (ω_0, ω_n and ζ_f) define the filter IRF in (4.21).

4.8 Parameter Identification

As shown above, the temporal and spectral characteristics of the model are completely separable. Specifically, the modulating function $q(t)$ describes the evolving RMS of the process, whereas the filter IRF $h[t-\tau, \theta(\tau)]$ controls the evolving frequency content of the process. This means that the parameters of the modulating function and of the filter can be independently identified by matching the corresponding statistical characteristics of a target accelerogram.

4.8.1 Identification of parameters in the modulating function

Let $\lambda = (T_0, T_1, T_2, \sigma_{max}, \alpha, \beta)$ denote the parameters of the modulating function, so that $q(t) = q(t, \lambda)$. For a target accelerogram, $a(t)$, we determine λ by matching the expected cumulative energy of the process, $E_x(t) = (\frac{1}{2}) \int_0^t q^2(\tau, \lambda) \mathrm{d}\tau$, with the cumulative energy in the accelerogram, $E_a(t) = (\frac{1}{2}) \int_0^t a^2(\tau) \mathrm{d}\tau$, over the duration of the ground motion, $0 < t < t_n$. This is done by minimizing the integrated squared difference between the two cumulative energy terms, i.e.

$$\overline{\lambda} = \arg\min_{\lambda} \int_0^{t_n} \left[\int_0^t q^2(\tau, \lambda) B(\tau) \mathrm{d}\tau - \int_0^t a^2(\tau) B(\tau) \mathrm{d}\tau \right]^2 \mathrm{d}t \tag{4.23}$$

where $B(t)$ is a weight function introduced to avoid dominance by the strong motion phase of the record, otherwise, the tail of the record is not well fitted. The function, $B(t) = \min \left[\frac{[\max_t q_0^2(t)]}{q_0^2(t)}, 5 \right]$, where $q_0(t)$ is the modulating function obtained in a

prior optimization without the weight function. The objective function in (4.23), which was earlier used by Yeh and Wen [22] without the weight function, has the advantage that the integral $\int_0^t a^2(\tau)B(\tau)\mathrm{d}\tau$ is a relatively smooth function so that no artificial smoothing is necessary.

As a measure of the error in fitting to the cumulative energy of the accelerogram, we use the ratio

$$\epsilon_q = \frac{\int_0^{t_n} |E_x(t) - E_a(t)|\,\mathrm{d}t}{\int_0^{t_n} E_a(t)\mathrm{d}t} \tag{4.24}$$

The numerator is the absolute area between the two cumulative energy curves and the denominator is the area underneath the energy curve of the target accelerogram.

4.8.2 Identification of filter parameters

The parameters ω_0 and ω_n defining the time-varying frequency of the filter (4.22) and parameters defining its damping ratio ζ_f control the predominant frequency and bandwidth of the process. Since these parameters have interacting influences, ω_0 and ω_n are first determined while keeping the filter damping, ζ_f a constant. For a given ζ_f, the parameters ω_0 and ω_n are identified by matching the cumulative expected number of zero-level up-crossings of the process, i.e. $\int_0^t \nu(0^+,\tau)\mathrm{d}\tau$ with the cumulative count $N(0^+,t)$ of zero-level up-crossings in the target accelerogram for all t, $0 < t < t_n$. This is accomplished by minimizing the mean-square error

$$[\hat{\omega_0}(\zeta_f), \hat{\omega_n}(\zeta_f)] = \arg\min \int_0^{t_n} \left[\int_0^t \nu(0^+,\tau)r(\tau)\mathrm{d}\tau - N(0^+,t)\right]^2 \mathrm{d}t \tag{4.25}$$

where $r(\tau)$ is an adjustment factor as described below. $\nu(0^+,\tau)$ is an implicit function of the filter characteristics ω_f and ζ_f and therefore, ω_0 , ω_n and ζ_f. The same is true for $r(\tau)$. The calculation of $\int_0^t \nu(0^+,\tau)\mathrm{d}\tau$ is as described in Section 4.6.

When a continuous-parameter stochastic process is represented as a sequence of discrete-time points of equal intervals Δt, the process effectively loses its content

beyond a frequency approximately equal to $\frac{\pi}{2\Delta t}$ rad/s. This truncation of high-frequency components results in undercounting of level crossings. The undercount per unit time, denoted r, is a function of Δt as well as the frequency characteristics of the process. So r, is a function of Δt, ω_f and ζ_f. Approximate expressions for r are

$$r(\tau) = \begin{cases} 1 - 0.0005\left(\omega_f(\tau) + \zeta_f(\tau)\right) - 0.00425\omega_f(\tau)\zeta_f(\tau) & \text{when } \Delta t = 0.01s \\ 1 - 0.01\zeta_f(\tau) - 0.009\omega_f(\tau)\zeta_f(\tau) & \text{when } \Delta t = 0.02s \end{cases} \tag{4.26}$$

Since digitally recorded accelerograms are available only in the discretized form, the count $N(0^+, t)$ underestimates the true number of crossings of the target accelerogram by the factor $r(\tau)$ per unit time. Hence, to account for this effect, we must multiply the rate of counted up-crossings by the factor $\frac{1}{r(\tau)}$. However, $r(\tau)$ depends on the predominant frequency and bandwidth of the accelerogram. So, it is more convenient to adjust the theoretical mean up-crossing rate (the first term inside the square brackets in (4.25) by multiplying it by the factor $r(\tau)$.

In order to solve (4.25), the filter damping ratio, ζ_f which controls the bandwidth of the process is selected. Corresponding ω_0 and ω_n are calculated. Measure of the error in fitting to the cumulative number of zero-level up-crossings is given by

$$\epsilon_w = \frac{\int_0^{t_n} \left| \int_0^t \nu(0^+, \tau, \hat{\omega_0}, \hat{\omega_n}, \zeta_f) r(\tau) \mathrm{d}\tau - N(0^+, t) \right| \mathrm{d}t}{\int_0^{t_n} N(0^+, t) \mathrm{d}t} \tag{4.27}$$

The optimum value of ζ_f can be chosen by comparing the cumulative number of negative maxima and positive minima of the target accelerogram and the fitted model.

Table 4.1: Summary of parameters of the stochastic ground motion model

S. No.	Parameter	Description
1	T_0	Starting time of the process
2	T_1	Starting time of the strong motion phase
3	T_2	Ending time of the strong motion phase
4	σ_{max}	RMS value of acceleration in strong motion phase
5	α	Parameter that shape the decaying end
6	β	parameter that shape the decaying end
7	ω_0	Filter frequency at time, T_0
8	ω_n	Filter frequency at time, T_n
9	ζ_f	Filter damping ratio
10	t_n	Total duration of ground motion
11	Δt	Time steps required

4.9 Summary of Parameters

A summary of all the parameters required to generate a ground motion using the above described process is given in a tabular form in the Table 4.1. The first nine parameters are already described. Two more parameters are required. One is the total duration of the ground motion T_n, the other is the time steps in the accelerogram represented by Δt.

Chapter 5

Stochastic Simulation of Ground Motions

5.1 Introduction

A method to generate an ensemble of artificial earthquake ground motions is described in this chapter. The method is based upon the stochastic ground motion model described in the previous chapter. A database of recorded earthquake ground motions is created. In the next step, the nine parameters required to depict a particular ground motion is found out for all the ground motions in the database. Probability distributions are created for the parameters of all the earthquakes in the database. Now, the parameters required by the stochastic ground motion model to simulate ground motions are obtained from the distributions. Monte Carlo simulations is used to generate an ensemble of ground motions.

5.2 Database of Recorded Time Histories

A database of recorded earthquake accelerograms is created. The earthquakes are selected arbitrarily. Earthquakes with intensity varying from moderate to high that have occurred throughout the world in the past century are chosen. The chosen

earthquakes have occurred on different site conditions and have different characteristics. Earthquake data are collected from reliable sources like National Geophysical Data Center (NGDC), USA [1]and The European Strong Motion Database (ESD) [2].

The details of the earthquakes in the database is given in Table 5.1. All the time histories are edited to an uniform format. Further, it is shown that there is no correlation between the earthquakes by finding the average of the power spectral densities of all the earthquakes. The plot as shown in Figure 5.1 shows that the spectrum resembles that of a white noise.

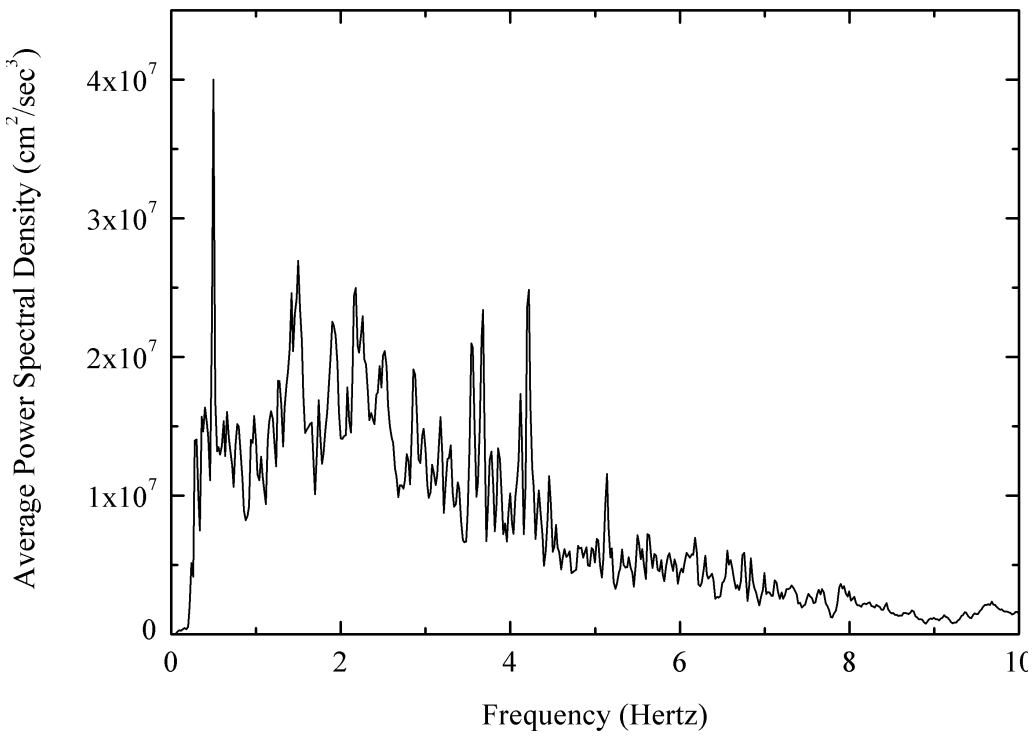

Figure 5.1: Plot showing the average power spectral density vs frequency

[1]http://www.ngdc.noaa.gov/hazard/data/cdroms/ accessed in October 2009.
[2]http://www.isesd.cv.ic.ac.uk/ESD/frameset.htm accessed in October 2009.

Table 5.1: Details of earthquakes in the database

S. No.	Earthquake	Event Date	Recording Station	Component	PGA (g)	Duration (sec)
1	Imperial Valley	May 18th, 1940	El Centro	0	0.341	53.76
2	Loma Prieta	October 18th, 1989	Los Gatos Presentation Centre	90	0.596	25.005
3	Northridge	January 17th, 1994	Sylmar Converter Station	360	0.827	60
4	Kobe	January 17th, 1995	JMA	NS	0.818	150
5	Mexico City	September 19th, 1995	Station 1	180	0.168	180.12
6	Kern County, CA	July 21st, 1952	Taft Lincoln School Tunnel	S69E	0.176	54.4
7	Koyna Dam No 02	September 13th, 1967	Koyna Dam, Shear Zone Gallery	Long	0.16	10.7
8	Koyna Dam No 06	December 10th, 1967	Koyna Dam, 1A Gallery	Long	0.48	10.72
9	Uttarkashi	October 19th, 1991	Uttarkashi	N15W	0.237	39.92
10	Tangshan	July 28th,1976	Beijing Hotel Point 1 Basement	EW	0.065	49.23
11	Romania - Vrancea	March 4th, 1977	Incerc-Bucharest	NS	0.194	40.16
12	Vrancea	August 30th, 1986	Bacau	NS	0.088	42.61
13	Vrancea	May 30th, 1990	Bacau	EW	0.122	42.22
14	Vrancea	May 31st, 1990	Carcaliu	NS	0.059	37.54
15	San Salvador	October 10th, 1986	Inst. Urban Construc.	90	0.379	11.54
16	Northwest California	October 7th, 1951	Ferndale City Hall	N46W	0.109	55.9
17	Kern County, CA	July 21st, 1952	Taft Lincoln School Tunnel	S69E	0.176	54.4
18	Eureka	December 21st, 1954	Eureka Federal Bldg	N79E	0.252	75.98
19	San Jose	September 04th, 1955	San Jose Bank of America Basement	N59E	0.105	51.76
20	El Alamo, Baja California	February 09th, 1956	El Centro Site Imperial Valley Irrig District	S90W	0.05	89.98
21	Coalinga	May 02nd, 1983	Slack Canyon	N45E	0.169	60.02
22	San Francisco	March 22nd, 1957	San Francisco Golden Gate Park	S80E	0.102	39.88
23	Hollister	April 08th, 1961	Hollister City Hall	N89W	0.175	40.5
24	Helena, Montana	October 31st, 1935	Helena Montana Carroll College	S00W	0.143	50.92
25	Borrego Mountain	April 08th, 1968	El Centro Site Imperial Valley Irrig District	S00W	0.127	87.42
26	Long Beach	March 10th, 1933	Vernon CMD Building	N82W	0.151	98.44

Continued on next page

Table5.1 – continued from previous page

S. No	Earthquake	Event Date	Recording Station	Component	PGA (g)	Duration (sec)
27	Southern California	October 02ndnd, 1933	Hollywood Storage Building Penthouse	N90E	0.085	89.66
28	Lower California	December 30th, 1934	El Centro Imperial Valley	S90W	0.179	90.24
29	1st Northwest California	September 11th, 1938	Ferndale City Hall	N45E	0.14	71.38
30	2nd Northwest California	February 09th, 1941	Ferndale City Hall	N45E	0.061	67.28
31	Western Washington	April 13th, 1949	Olympia, Washington HWY Test Lab	N86E	0.274	89.06
32	Northern California	September 22nd, 1952	Ferndale City Hall	S46E	0.074	58
33	Wheeler Ridge, California	January 12th, 1954	Taft Lincoln School Tunnel	N21E	0.063	65.4
34	Puget Sound, Washington	April 29th, 1965	Olympia, Washington HWY Test Lab	S86W	0.194	81.96
35	Parkfield	June 27th, 1966	Cholame, Shandon	N65E	0.479	43.66
36	San Fernando	February 9th, 1971	Pacoima Dam	S74W	1.054	41.72
37	Mammoth Lakes	May 25th, 1980	Convict Creek	180	0.392	65
38	Morgan Hill	April 24th, 1984	Halls Valley	240	0.305	60
39	Whittier	October 1st, 1987	Los Angeles - Obregon Park	360	0.42	40
40	Mt. Diablo, Livermore	January 24th, 1980	Del Valle Dam (Toe)	S66W	0.25	31.04
41	Westmorland	April 26th, 1981	Parachute Test Facility, El Centro	N45W	0.144	41.74
42	Off coast of Portugal	February 28th, 1969	Lisbon- Tejo	EW	0.025	25.94
43	Friuli	May 06th, 1976	Tolmezzo-Diga Ambiesta	NS	0.35	36.53
44	Gazli	May 17th, 1976	Karakyr Point	EW	0.706	13.02
45	Friuli (aftershock)	September 15th, 1976	Breginj-Fabrika IGLI	EW	0.495	9.98
46	Bucharest	March 04th, 1977	Bucharest Building Research Institute	NS	0.197	16.13
47	Ardal	April 06th, 1977	Naghan 1	Long	0.89	11.46
48	Basso Tirreno	April 15th, 1978	Patti-Cabina Prima	EW	0.158	30.84
49	Volvi	June 20th, 1978	Thessaloniki-City Hotel	EW	0.143	30.59
50	Tabas	September 16th, 1978	Tabas	N16W	1.08	63.41
51	Montenegro	April 15th, 1979	Petrovac-Hotel Oliva	NS	0.445	48.22
52	Campano Lucano	November 23rd, 1980	Brienza	NS	0.222	30.15
53	Alkion	February 24th, 1981	Korinthos-OTE Building	N120	0.303	41.86

Continued on next page

Table5.1 – continued from previous page

S. No	Earthquake	Event Date	Recording Station	Component	PGA (g)	Duration (sec)
54	Panisler	October 30th, 1983	Horasan-Meteoroloji Mudurlugu	EW	0.157	28.01
55	Spitak	December 07th, 1988	Gukasian	EW	0.176	22.98
56	Manjil	June 20th, 1990	Abhar	N33W	0.204	29.48
57	Erzincan	March 13th, 1992	Erzincan-Meteorologij Mudurlugu	N279	0.502	20.74
58	South Aegean	May 23rd, 1994	Chania-OTE Building	TRAN	0.056	30.5
59	Bitola	September 01st, 1994	Florina-Cultural Center	257	0.079	21.74
60	Kozani	May 13th, 1995	Kozani-Prefecture	342	0.203	29.37
61	Aigion	June 15th, 1995	Patra-San Dimitrios Church	110	0.091	39.5
62	Dinar	October 01st, 1995	Dinar-Meteoroloji Mudurlugu	WE	0.313	27.95
63	Gulf of Abaka	November 22nd, 1995	Eilat	EW	0.089	59.99
64	Umbria Marche	September 26th, 1997	Assisi-Stallone	N18E	0.183	29.42
65	Kalamata	October 13th, 1997	Koroni-Town Hall (Library)	35	0.118	48.6
66	Strofades	November 18th, 1997	Zakynthos-OTE Building	140	0.128	65.43
67	Adana	June 27th, 1998	Ceyhan-Tarim Ilce Mudurlugu	EW	0.264	29.18
68	Izmit	August 17th, 1999	Duzce-Meteoroloji Mudurlugu	WEST	0.354	27.17
69	Ano Liosia	September 07th, 1999	Athens 3 (Kallithea District)	N136	0.301	39.05
70	Duzce	November 12th, 1999	IRIGM Station No. 496	NS	1.019	29.99
71	South Iceland	June 17th, 2000	Flagbjarnarholt	TRAN	0.331	76.78
72	Ionian	April 24th, 1988	Lefkada-Hospital	155	0.27	21.63
73	Etolia	May 18th, 1988	Valsamata-Seismograph Station	TRAN	0.173	25.42
74	Off coast of Levkas	August 24th, 1988	Lefkada-Hospital	TRAN	0.236	21.59
75	Kyllini	October 16th, 1988	Amaliada-OTE Building	N170	0.153	30.51
76	Chenoua	October 29th, 1989	Cherchell	N180	0.283	23.98
77	Aigion	May 17th, 1990	Aigio-OTE Building	N150	0.195	16.13
78	Sicilia-Orientale	December 13th, 1990	Catania-Piana	NS	0.248	43.44
79	Kefallinia island	January 23rd, 1992	Argostoli-OTE Building	59	0.222	20.69
80	Pyrgos	March 26th, 1993	Pyrgos-Agriculture Bank	TRN	0.425	25.59

Continued on next page

Table5.1 – continued from previous page

S. No	Earthquake	Event Date	Recording Station	Component	PGA (g)	Duration (sec)
81	Patras	July 14th, 1993	Patra-San Dimitrios Church	TRAN	0.333	29.28
82	Komilion	February 25th, 1994	Lefkada-OTE Building	TRAN	0.195	27.03
83	Mt. Hengill Area	August 24th, 1997	Hveragerdi-Church	LONG	0.169	35.98
84	Umbria	September 03rd, 1997	Nocera Umbra	NS	0.289	26.98
85	Oelfus	November 14th, 1998	Hveragerdi-Church	TRAN	0.231	35.98
86	Ancona	February 04th, 1972	Genio-Civile	EW	0.123	7.7
87	Azores	November 23rd, 1973	San Mateus	NS	0.268	19.2
88	Denizli	August 19th, 1976	Denizli-Bayindirlik ve Iskan Mudurlugu	NS	0.338	15.85
89	Izmir	December 16th, 1977	Izmir-Meteoroloji Istasyonu	NS	0.205	6.5
90	Preveza	March 10th, 1981	Preveza-OTE Building	NS	0.14	18.3
91	Levkas	May 27th, 1981	Lefkada-OTE Building	N25E	0.117	15.99
92	NE of Banja Luka	August 13th, 1981	Banja Luka-Institut za Ispitivanje Materijala	NS	0.434	32.3
93	Heraklio	March 19th, 1983	Heraklio-Prefecture	EW	0.178	20.3
94	Ierissos	August 26th, 1983	Ierissos-Police Station	TRAN	0.179	21.09
95	Provadja	November 10th, 1983	Provadja-Clock Tower	TRAN	0.254	12.48
96	Arpiola	March 22nd, 1984	Tregnago	WE	0.119	11.23
97	Balikesir	March 29th, 1984	Balikesir-Bayindirlik ve Iskan Mudurlugu	NS	0.204	7.83
98	Baskoy	August 12th, 1985	Kigi-Meteoroloji Mudurlugu	SN	0.152	10.01
99	Kalamata	September 13th, 1986	Kalamata-OTE Building	N10W	0.267	29.86
100	SE of Tirana	January 09th, 1988	Tirana-Seismological Observatory	EW	0.403	11.96

5.3 Determination of Parameters

The nine parameters of the stochastic ground motion model as described in Section 4.7 are found out for each of the earthquakes in the database. The two additional parameters that are required are the time duration T_n and the time steps Δt. T_n is known from the time history and Δt is taken as 0.02 sec for all the earthquakes.

As the temporal and spectral nonstationarities are separable in the considered stochastic ground motion model, the parameters of the modulating function and the parameters of the filter are found out separately. The results are shown for one accelerogram. The accelerogram chosen is the October 18th, 1989 Loma Prieta earthquake's 90 component recorded at Los Gatos Presentation Centre.

5.3.1 Parameters in the modulating function

The six parameters required for the modulating function can be obtained by solving (4.23) by using an optimization technique. The minimum of the unconstrained multivariable function in (4.23) is obtained by using Nelder-Mead simplex algorithm [28]. A MATLAB code is developed for this purpose.

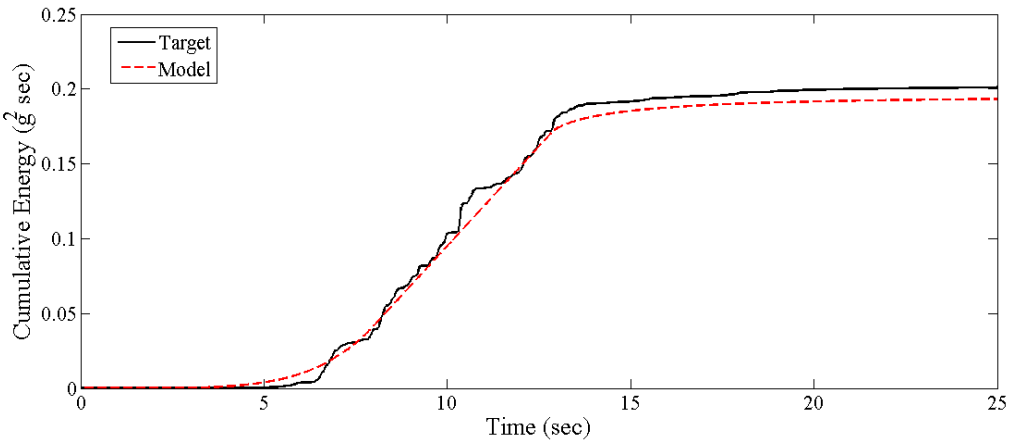

Figure 5.2: Cumulative energies in the target accelerogram and the fitted model

Figure 5.2 compares the two energy terms $2E_x(t) = \int_0^t q^2(\tau, \lambda)\mathrm{d}\tau$ and $2E_a(t) = \int_0^t a^2(\tau)\mathrm{d}\tau$, described in Section 4.7. It is seen that the fit is good at all the time

Table 5.2: Values of parameters in the modulating function

S. No.	Parameter	Value
1	T_0	0.072932 sec
2	T_1	8.0154 sec
3	T_2	12.88 sec
4	σ_{max}	0.16308 g
5	α	0.80585 sec^{-1}
6	β	0.44846
7	t_n	25 sec
8	Δt	0.02 sec

points. The error is minimised. The parameters obtained after optimization is summarized in Table 5.2.

5.3.2 Parameters in the filter

Using the same method of optimization mentioned in Section 5.3.1, the parameters in the filter is obtained by solving (4.25). To solve (4.25), first a value of ζ_f is assumed. ζ_f is considered to be constant for the entire duration of the earthquake. After obtaining the values of ω_0 and ω_n, seperate optimization is done by minimizing the difference between the cumulative count of negative maxima and positive minima of the target and the model. The values of ω_0 and ω_n are kept unchanged as it is found that there is no big variation. Now, the exact value of ζ_f is known. The values of ω_0 and ω_n are found corresponding to the final ζ_f. For the considered accelerogram it is found to be 0.8.

Shown in Figure 5.3 is the cumulative count of negative maxima and positive minima as a function of time for the Loma Prieta, 1989 record as well as the estimated values of the same quantity of the model with damping ration $\zeta_f = 0.8$. The slope of these lines should be considered as the instantaneous measure of bandwidth.

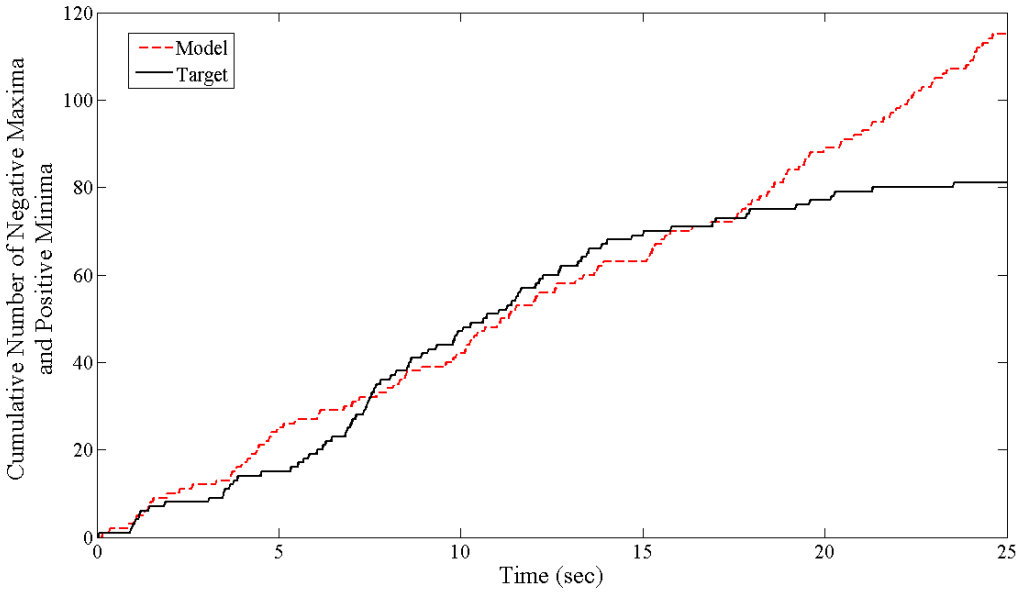

Figure 5.3: Cumulative count of negative maxima and positive minima

Table 5.3: Values of parameters in the filter

S. No.	Parameter	Value
1	ω_0	30.297 rad/sec
2	ω_n	10.075 rad/sec
3	ζ_f	0.8

The parameters in the filter obtained after optimization is summarized in Table 5.3.

Shown in Figure 5.4 is the cumulative number of zero-level up-crossings as a function of time for the Loma Prieta, 1989 record as well as the estimated values of the same quantity of the model. It is seen that the fit is good at all the time points.

5.4 Simulation of a Target Accelerogram

After finding out all the parameters, an accelerogram can be simulated by using the process described in the previous chapter. Simulated accelerogram has similar

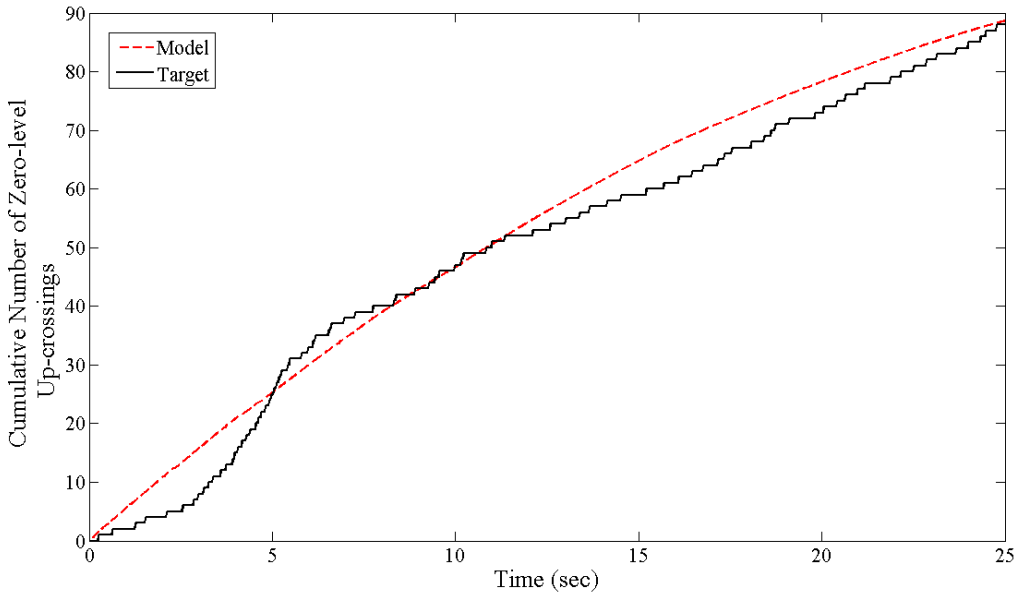

Figure 5.4: Cumulative number of zero-level up-crossings in the target accelerogram and model

characteristics but it will not be an exact replica of the target accelerogram. The target accelerogram and a simulation is shown in the Figure 5.5.

To get more accurate simulations, the damping ratio of the filter ζ_f should be considered as varying at various intervals of time. For simplicity, the damping ratio of the filter ζ_f is considered as constant throughout the entire duration of the earthquake.

Since we had described the ground acceleration as a filtered white noise process which has a non-zero spectral density at zero frequency, the integral of the process (the ground velocity or displacement) has infinite spectral density at zero frequency. Because of this property, the variances of the velocity and displacement processes keep on increasing even after the acceleration has vanished. This is contrary to (baseline-corrected) accelerograms, which have zero residual velocity and displacement at the end of the record. To overcome this problem, it is necessary to adjust the low-frequency content of the stochastic model using a high-pass filter. This is not done in the present work.

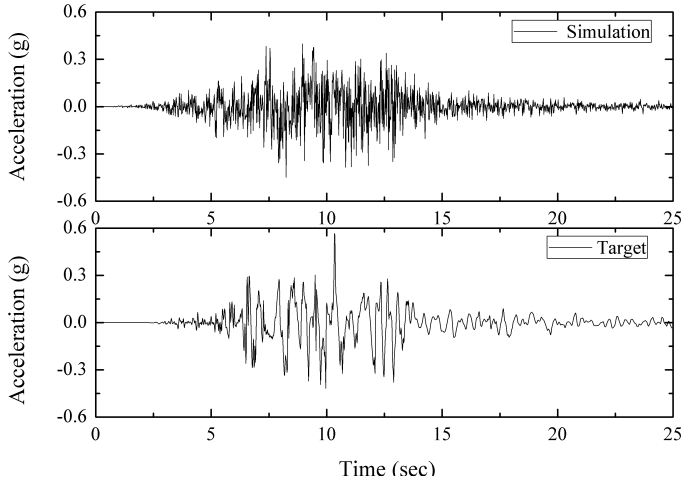

Figure 5.5: Target accelerogram and a simulation using the fitted model

5.5 Distribution of Parameters

After identifying the model parameter values by fitting to each recorded ground motion in the database, a probability distribution is assigned to the sample of values of each parameter. Now, there are 100 sets of parameters representing the 100 earthquakes. The time steps Δt is kept constant for all the 100 earthquakes. Distribution models are assigned to each of the 10 parameters.

5.5.1 Pearson distributions

This approach proposed by Karl Pearson [29], seeks to ascertain a family of distributions that will satisfactorily represent observed data. Several important distributions satisfy a difference equation that can be expressed in the form [30]

$$\frac{dp(x)}{dx} = \frac{a_0 + a_1 x}{b_0 + b_1 x + b_2 x^2} p(x) \tag{5.1}$$

where $p(x)$ is the probability density function (PDF) at any x. a_i and b_i, $i = 0, 1, 2$ are constants calculated from central normalised statistical moments. They are represented as

$$a_0 = \mu_3(\mu_4 + 3) \tag{5.2a}$$

$$a_1 = 10\mu_4 - 18 - 6\mu_3^2 \tag{5.2b}$$

$$b_0 = 3\mu_3^3 - 4\mu_4 \tag{5.2c}$$

$$b_1 = -\mu_3(\mu_4 + 3) \tag{5.2d}$$

$$b_2 = 3\mu_3^2 - 2\mu_4 + 6 \tag{5.2e}$$

The moments μ_k are given by

$$\mu_k = \frac{m_k}{\sigma^k} = \frac{1}{N\sigma^k}\sum_{i=1}^{N}[x_i - E(x)]^k = \frac{1}{N}\sum_{i=1}^{N}\left\langle\frac{[x_i - E(x)]}{\sigma}\right\rangle^k \tag{5.3}$$

Wwhere

$$Ex = \frac{1}{N}\sum_{i=1}^{N} x_i \tag{5.4a}$$

$$m_k = \frac{1}{N}\sum_{i=1}^{N}[x_i - E(x)]^k \tag{5.4b}$$

The moment μ_1 is the mean, μ_2 is the variance, μ_3 is the skewness and μ_4 is the kurtosis. The determinant D is given by

$$D = 4b_0b_2 - b_1^2 \tag{5.5}$$

The main types of distribution are distinguished based on the roots of the quadratic in the denomonator of (5.1) and the value of b_2. Two of the important types of distributions are explained as examples.

Pearson Type I

When $D < 0$ and $b_2 \neq 0$, the distribution is classified as Pearson type I which is also called as the generalised β distribution. For this type, the PDF $p(x)$is given by

$$p(x) = \begin{cases} k_n(x - x_1)^r(x_2 - x)^s & x_1 \leq x \leq x_2 \\ \\ 0 & \text{otherwise} \end{cases} \tag{5.6}$$

where

$$x_{1,2} = -\frac{b_1 \pm z}{2b_2} \tag{5.7a}$$

$$r = \frac{a_0 + a_1 x_1}{b_2(x_1 - x_2)} > -1 \tag{5.7b}$$

$$s = \frac{a_0 + a_1 x_2}{b_2(x_2 - x_1)} > -1 \tag{5.7c}$$

here $z = \sqrt{-D}$ and k_n is calculated such that $\int_{x_1}^{x_2} p(x)dx = 1$.

Pearson Type IV

When $D > 0$ and $b_2 \neq 0$, the distribution is classified as Pearson type IV. For this type, the PDF $p(x)$is given by

$$p(x) = K_n[a^2 + (x + x_0)^2]^{-u} e^{-v \arctan(\frac{x+x_0}{a})} \tag{5.8}$$

where

Table 5.4: Statistical characteristics of the parameter data

Parameter	Mean	Standard Deviation	Lowest Value	Highest Value
T_0	0.03	0.06	0.00	0.18
T_1	2.91	5.25	0.00	43.95
T_2	10.52	8.71	0.82	43.90
T_n	40.88	28.40	6.50	180.12
α	1.46	1.77	0.01	8.47
β	1.24	1.31	0.01	7.67
σ_{max}	0.08	0.07	0.01	0.33
ω_0	31.89	13.28	8.86	73.26
ω_n	15.15	13.43	0.00	56.59
ζ_f	0.51	0.23	0.10	0.90

$$x_0 = \frac{b_1}{2b_2} \tag{5.9a}$$

$$u = \frac{-a_1}{2b_2} > 0 \tag{5.9b}$$

$$v = \frac{2b_2(1-u)}{z} \tag{5.9c}$$

$$a = \frac{z}{2b_2} \tag{5.9d}$$

here $z = \sqrt{D}$ and k_n is calculated such that $\int_{-\infty}^{\infty} p(x)dx = 1$.

5.5.2 Distribution of model parameters

It is found that the data of all the 10 parameters are effectively fitted by β distribution. A MATLAB code is written to determine the parameters required in (5.6). The statistical details of the data of each parameter is given in Table 5.4.

Figure 5.6 shows the normalized frequency diagrams of the fitted model parameters for the entire dataset with the fitted probability density functions (PDFs) superimposed. All the parameters have β distribution and the parameter values of

Table 5.5: Details of the β PDF of all the parameters

Parameter	**Data**	x_1	x_2	r	s	k_n
T_0	linear	0.01	0.16	-0.46	2.53	317
T_1	linear	1.72	55.82	-0.80	7.78	4.98E-15
T_2	log	-0.59	1.84	4.88	2.83	1.75E-01
T_n	log	-0.34	2.68	14.50	8.64	4.51E-05
α	linear	-0.04	13.33	0.28	9.13	4.16E-11
β	linear	0.06	47.70	0.66	63.87	1.25E-107
σ_{max}	log	-2.61	0.28	6.48	7.50	6.30E-03
ω_0	linear	9.74	141.16	2.02	13.90	2.95E-33
ω_n	linear	-2.96	67.00	0.61	3.62	3.17E-09
ζ_f	linear	0.05	1.02	0.59	0.73	3.61

their distribution is listed in Table 5.5.

5.6 Generation of an Ensemble of Ground Motions

A cluster of earthquake ground motions is produced. This is done by randomly selecting the parameters of the stochastic ground motion model. Initially 10000 samples of each parameter is arbitrarily chosen from the distributions of the particular parameter. From this pool of samples, 5000 sets of parameters which satisfy the conditions specified in Section 4.7 are chosen.

Using this 5000 sets of parameters, 5000 artificial ground motions are generated. This cluster of earthquakes represents a completely random choice of ground motions.

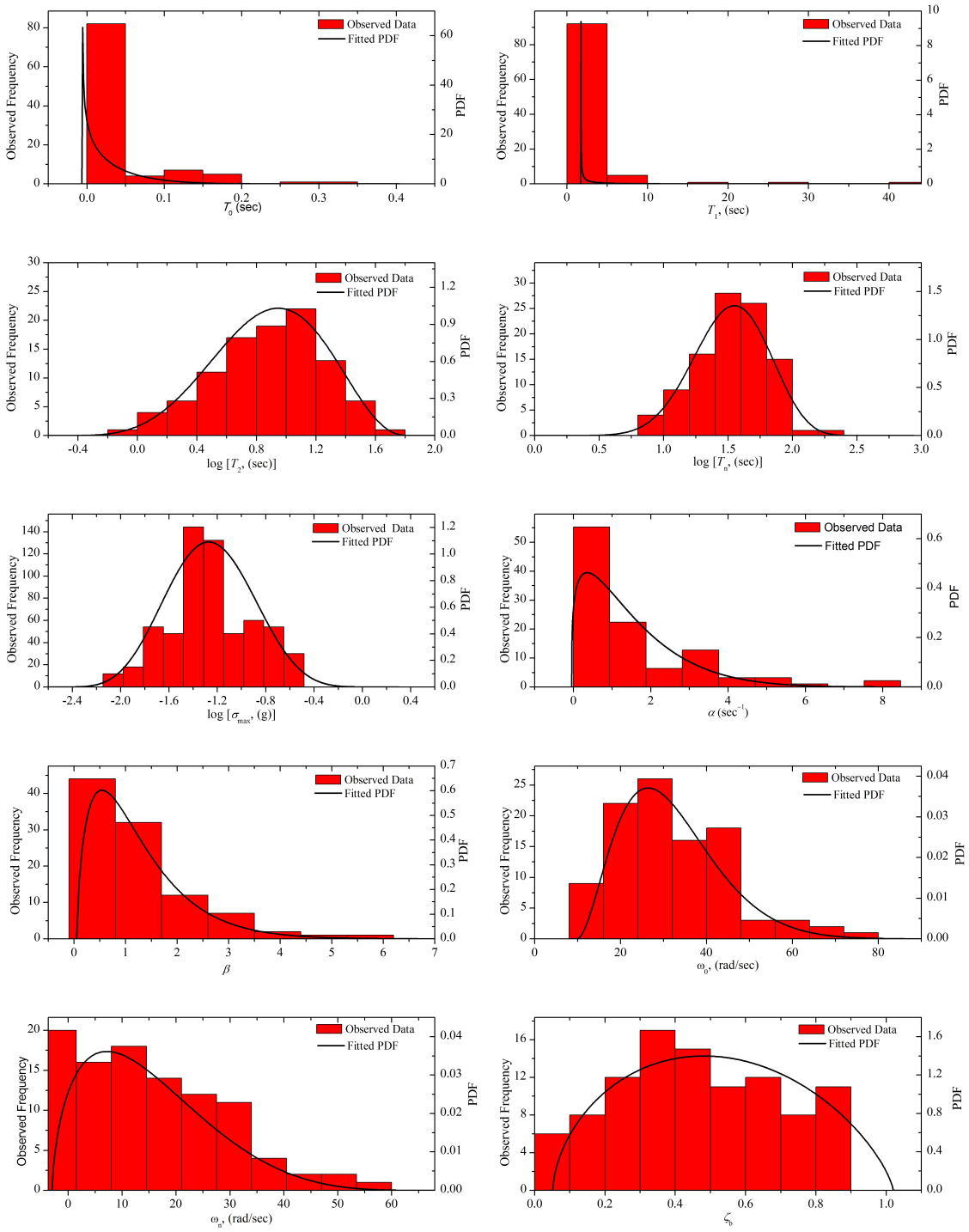

Figure 5.6: PDF of parameters superimposed on observed normalized frequency diagrams

Chapter 6

Stochastic Response of an Isolated Building

6.1 Introduction

The stochastic response of the base-isolated building structure is calculated by using direct Monte Carlo simulations. The uncertainty in the characteristics of the ground motion is considered and all the structural parameters are considered to be deterministic. Response analysis, reliability analysis and parametric studies are presented in this chapter. The deterministic analysis procedure for each simulation is as described in the Chapter 3.

6.2 Response Quantities

The response quantities of interest are the absolute peak value of the acceleration at the top floor, hereinafter simply referred as top floor acceleration and the peak value of the isolator displacement hereinafter simply referred as isolator displacement.

To perform the response analysis, a total of 5000 artificial earthquakes are simulated as described in Section 5.6. Deterministic analysis is performed for each simulation and their corresponding response quantities are calculated. The deter-

Table 6.1: Summary of parameters of the isolator for stochastic response

S. No.	Parameter	Value
1	Ratio of floor mass to isolator mass	1:1
2	Damping Ratio of the isolator, ζ_b	0.1
3	Time period of the isolator, T_b	2.0 sec
4	Design Displacement, D	40 cm
5	Yield displacement, q	2.5 cm

ministic results are then processed to find the peak values, root mean square (RMS) values and distributions of the response quantities.

While calculating the responses, the parameters of the structure are kept unchanged. The parameters are as given in Table 3.1. The parameters of the isolator considered are tabulated in Table 6.1.

The distributions of the responses are calculated. The type of the distribution is found out by using Pearson distributions as described in Section 5.5. The parameters of the distribution are calculated by using MATLAB functions which use the maximum likelihood estimates (MLE) to find the parameters of the distribution. The top floor acceleration is found to be fitted effectively by using beta distribution and the isolator displacement is effectively fitted by generalized pareto distribution.

The PDFs of the response quantities are plotted and superimposed with their observed frequency diagrams as shown in Figure 6.1. The cumulative distribution function (CDF) is plotted for both the response quantities and is shown in Figure 6.2.

The statistical characteristics of the response quantities are tabulated in Table 6.2. For the considered parameters, the extreme top floor acceleration is found to be 0.89g and the extreme isolator displacement is found to be 92 cm. Their corresponding root mean square values (RMS) are 0.185g and 9.122 cm.

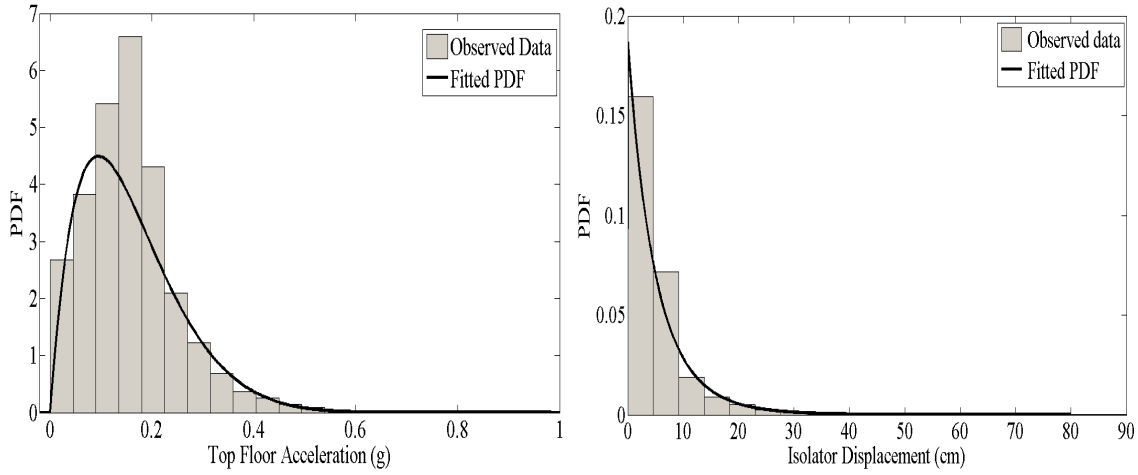

Figure 6.1: PDF of response quantities superimposed on observed normalized frequency diagrams

Table 6.2: Statistical details of the response quantities

Response quantity	**Lowest Value**	**Highest Value**	**Mean**	**Standard Deviation**	**Distribution Type**
Top floor acceleration (g)	1.47E-06	0.89	0.158	0.097	Beta
Isolator Displacement (cm)	0.004	92	5.873	6.981	Generalized Pareto

6.3 Extreme Earthquakes

An attempt is made to study the characteristics of the earthquakes which produce extreme responses. After 5000 simulations, 40 earthquakes were found to produce a top floor acceleration in excess of 0.4 g and 38 earthquakes were found to produce an isolator displacement in excess of 40 cm. It is seen that the base isolation is effective for more than 99 percent of the earthquakes generated.

After studying the parameters of the earthquakes that produce extreme responses, it is found that most of the earthquakes have a high value of RMS ground acceleration in the strong motion phase which is given by the parameter σ_{max}. How-

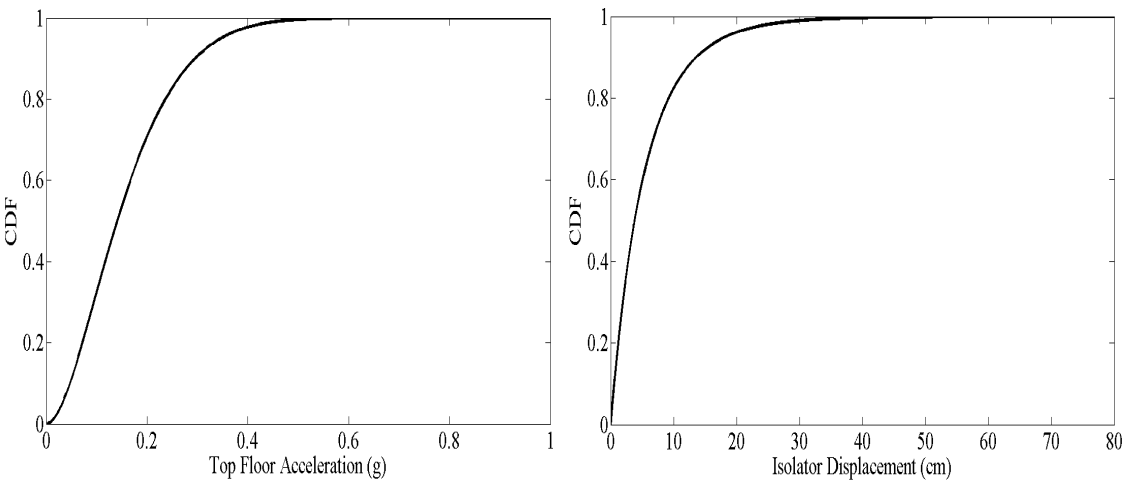

Figure 6.2: CDF of response quantities superimposed on observed normalized frequency diagrams

ever, there are some earthquakes with lesser value of σ_{max} which produce higher responses. This is due to the fact that the predominant frequency of the earthquake ground motion approaches the fundamental frequency of the base isolated building considered which induces the phenomenon of resonance.

To establish a relationship between the characteristics of these earthquakes and for a detailed study of these extreme earthquakes a huge number of simulations are required.

6.4 Reliability Analysis

6.4.1 Limit state

The probability of failure or limit state probability for this system is defined using a limit state function which is defined as the case where the top floor accelerations reach a 0.3 g acceleration level.

This can be formally stated with the limit state function

$$h(X) = 0.3 - |a_i| \tag{6.1}$$

where a_i is the peak acceleration of the top floor in g. Then, the probability of failure is defined as

$$P_f = P[h(X) \leq 0] \tag{6.2}$$

6.4.2 Probability of failure

The probability of failure is evaluated via Monte Carlo simulation by determining the number of realizations with $h(X) \leq 0$ and dividing that number by the total number of simulations.

The convergence of the probability of failure is demonstrated in Figure 6.3 where the isolator parameters $T_b = 2.0$ sec, $q = 2.5$ cm, $\zeta_b = 0.1$ and $D = 40$ cm. From Figure 6.3 it is seen that the probability of failure reaches a constant level at around 5000 simulations. Therefore, the convergence is achieved after 5000 simulations.

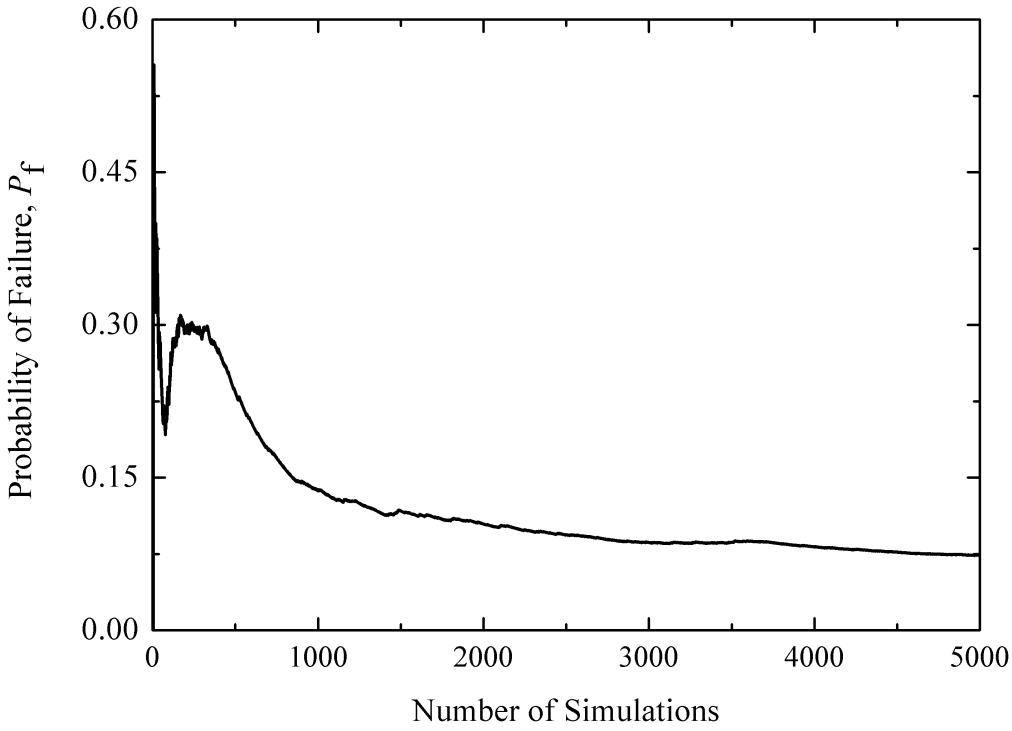

Figure 6.3: An example of convergence of probability of failure for the isolation system

Table 6.3: Peak values of the response of the structure: 200 simulations

	Top floor acceleration (g)				**Isolator displacement (cm)**			
	ζ_b=0.05	ζ_b=0.1	ζ_b=0.15	ζ_b=0.2	ζ_b=0.05	ζ_b=0.1	ζ_b=0.15	ζ_b=0.2
T_b=2 sec								
q=0.01 cm	0.93	1.03	1.20	1.41	83.28	65.54	46.40	44.47
q=2.5 cm	1.00	0.90	1.08	1.19	85.94	67.33	49.53	45.47
q=5 cm	1.00	0.87	0.90	1.06	86.79	69.25	55.10	45.54
T_b=3 sec								
q=0.01 cm	0.92	0.68	0.73	0.77	211.77	152.85	130.88	116.13
q=2.5 cm	0.92	0.70	0.60	0.61	210.52	158.47	136.64	122.41
q=5 cm	0.90	0.70	0.58	0.51	203.82	162.15	140.13	127.05
T_b=4 sec								
q=0.01 cm	0.82	0.63	0.55	0.52	339.29	284.78	247.10	217.39
q=2.5 cm	0.82	0.62	0.52	0.45	336.75	281.76	243.81	217.20
q=5 cm	0.79	0.63	0.51	0.42	332.92	284.08	241.39	222.21
T_b=5 sec								
q=0.01 cm	0.92	0.81	0.78	0.60	600.32	561.73	585.86	506.79
q=2.5 cm	0.90	0.78	0.74	0.60	596.43	563.25	572.98	489.96
q=5 cm	0.88	0.80	0.70	0.52	590.34	571.18	557.81	466.00

6.5 Parametric Studies

Analyses are conducted for different isolation periods and isolation damping ratios of isolation floor. Combinations of isolation periods of 2, 3, 4 and 5 sec, isolation damping ratios of 5%, 10%, 15% and 20% and isolator yield displacements of 0.01 cm, 2.5 cm and 5 cm are considered. Therefore, a total of 64 different structures are analysed. For every combination, the design displacement, D of the isolator is kept constant at 40 cm.

The peak top floor acceleration and peak isolator floor displacement, and the root mean square (RMS) values corresponding to these are in Tables 6.3 to 6.6. The RMS values of the response quantities for 200 simulations as shown in Table 6.4 and the corresponding values for 400 simulations shown in Table 6.6 are not varying significantly. So, the number of simulations for conducting parametric studies is fixed at 400.

Table 6.4: RMS values of the response of the structure: 200 simulations

	Top floor acceleration (g)				**Isolator displacement (cm)**			
	ζ_b=0.05	ζ_b=0.1	ζ_b=0.15	ζ_b=0.2	ζ_b=0.05	ζ_b=0.1	ζ_b=0.15	ζ_b=0.2
T_b=2 sec								
q=0.01 cm	0.35	0.49	0.60	0.70	19.74	13.03	9.92	8.51
q=2.5 cm	0.28	0.30	0.38	0.47	21.53	14.72	12.16	10.58
q=5 cm	0.29	0.28	0.32	0.37	23.12	16.65	13.96	12.57
T_b=3 sec								
q=0.01 cm	0.25	0.29	0.37	0.43	44.98	34.12	27.58	24.24
q=2.5 cm	0.22	0.19	0.19	0.21	45.94	35.51	29.82	26.67
q=5 cm	0.22	0.18	0.17	0.18	46.45	36.64	31.11	28.28
T_b=4 sec								
q=0.01 cm	0.20	0.21	0.26	0.30	71.09	58.19	50.76	47.14
q=2.5 cm	0.18	0.15	0.14	0.14	71.67	58.68	52.00	49.04
q=5 cm	0.18	0.15	0.13	0.13	71.90	59.02	52.95	50.55
T_b=5 sec								
q=0.01 cm	0.17	0.18	0.20	0.23	99.58	92.66	88.35	81.46
q=2.5 cm	0.16	0.14	0.13	0.12	99.44	92.90	88.56	82.48
q=5 cm	0.15	0.14	0.12	0.11	99.31	93.30	88.50	82.67

Table 6.5: Peak values of the response of the structure: 400 simulations

	Top floor acceleration (g)				**Isolator displacement (cm)**			
	ζ_b=0.05	ζ_b=0.1	ζ_b=0.15	ζ_b=0.2	ζ_b=0.05	ζ_b=0.1	ζ_b=0.15	ζ_b=0.2
T_b=2 sec								
q=0.01 cm	0.99	1.03	1.25	1.59	85.76	67.94	54.44	44.71
q=2.5 cm	1.00	0.90	1.08	1.27	87.79	75.98	61.18	45.47
q=5 cm	1.00	0.92	0.90	1.06	87.49	75.36	65.62	49.34
T_b=3 sec								
q=0.01 cm	0.92	0.68	0.73	0.77	211.77	152.85	130.88	116.13
q=2.5 cm	0.92	0.70	0.60	0.61	210.52	158.47	136.64	122.41
q=5 cm	0.90	0.70	0.58	0.51	203.82	162.15	140.13	127.05
T_b=4 sec								
q=0.01 cm	0.82	0.71	0.57	0.57	339.29	314.27	267.91	217.39
q=2.5 cm	0.83	0.70	0.58	0.45	337.17	317.72	266.66	217.20
q=5 cm	0.83	0.70	0.51	0.43	340.30	314.89	258.74	222.21
T_b=5 sec								
q=0.01 cm	0.92	0.81	0.78	0.60	600.32	561.73	585.86	506.79
q=2.5 cm	0.90	0.78	0.74	0.60	596.43	563.25	572.98	489.96
q=5 cm	0.88	0.80	0.70	0.52	590.34	571.18	557.81	466.00

Table 6.6: RMS values of the response of the structure: 400 simulations

	Top floor acceleration (g)				**Isolator displacement (cm)**			
	ζ_b=0.05	ζ_b=0.1	ζ_b=0.15	ζ_b=0.2	ζ_b=0.05	ζ_b=0.1	ζ_b=0.15	ζ_b=0.2
T_b=2 sec								
q=0.01 cm	0.33	0.47	0.58	0.67	17.97	11.74	8.97	7.63
q=2.5 cm	0.26	0.28	0.37	0.45	19.64	13.65	11.31	9.70
q=5 cm	0.27	0.27	0.30	0.35	21.12	15.57	13.20	11.61
T_b=3 sec								
q=0.01 cm	0.23	0.28	0.35	0.42	40.90	30.05	23.88	20.60
q=2.5 cm	0.20	0.17	0.18	0.20	41.73	31.50	25.92	22.99
q=5 cm	0.20	0.17	0.16	0.17	42.24	32.66	27.23	24.63
T_b=4 sec								
q=0.01 cm	0.18	0.21	0.25	0.29	65.58	53.73	45.62	40.69
q=2.5 cm	0.17	0.14	0.13	0.13	66.02	54.33	46.82	42.48
q=5 cm	0.17	0.14	0.12	0.12	66.33	54.70	47.69	43.94
T_b=5 sec								
q=0.01 cm	0.15	0.16	0.19	0.22	89.80	82.49	75.56	67.96
q=2.5 cm	0.14	0.12	0.11	0.10	89.88	82.67	75.90	69.20
q=5 cm	0.14	0.12	0.11	0.10	89.92	82.91	75.92	69.60

It is observed that the top floor acceleration decreases with the increase in the yield displacement of the isolator and the isolator displacement decreases with the increase in the yield displacement.

Figures 6.4, 6.5 and 6.6 show the variation of response quantities for different isolation periods, T_b and isolation damping ratios, ζ_b when the value of the yield displacement of the isolator, q is assumed as 0.01 cm, 2.5 cm and 5 cm respectively. It can be seen that the top floor acceleration decreases as the isolation time period increases. Also, the top floor acceleration decreases as the damping ratio increases. The displacement in the isolator increases as the time period increases, and decreases as the damping ratio increase.

The acceleration response decreases with increasing isolation periods. The smallest possible acceleration favors the selection of $T_b = 5$ sec for the isolation period. However, peak isolator displacement is high with long isolation periods. This prob-

lem can be solved by employing high damping. Therefore, the isolation system with a long isolation period and high damping is the most effective.

This design approach for the isolation system can help design engineers in designing reliable isolation systems.

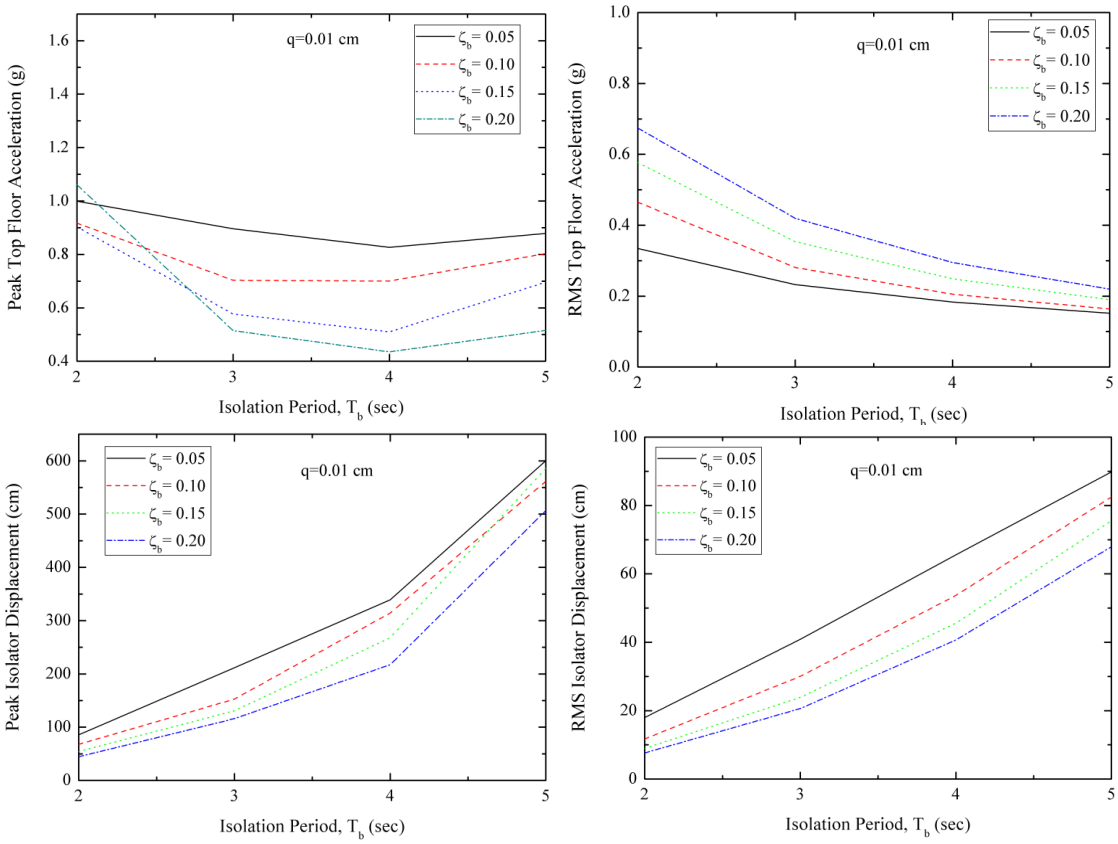

Figure 6.4: Variation of response quantities for different isolation periods, T_b and isolation damping ratios, ζ_b, $q = 0.01$ cm, 400 simulations

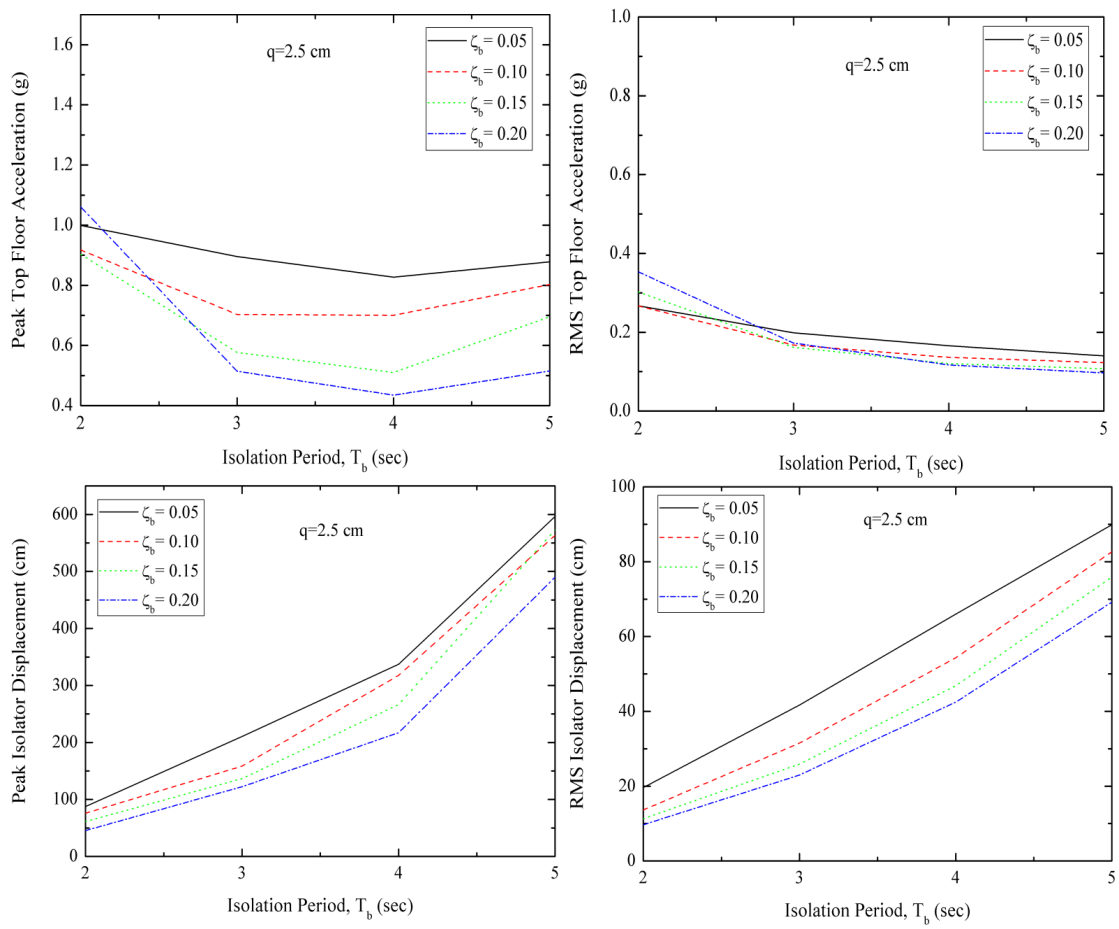

Figure 6.5: Variation of response quantities for different isolation periods, T_b and isolation damping ratios, ζ_b, $q = 2.5$ cm, 400 simulations

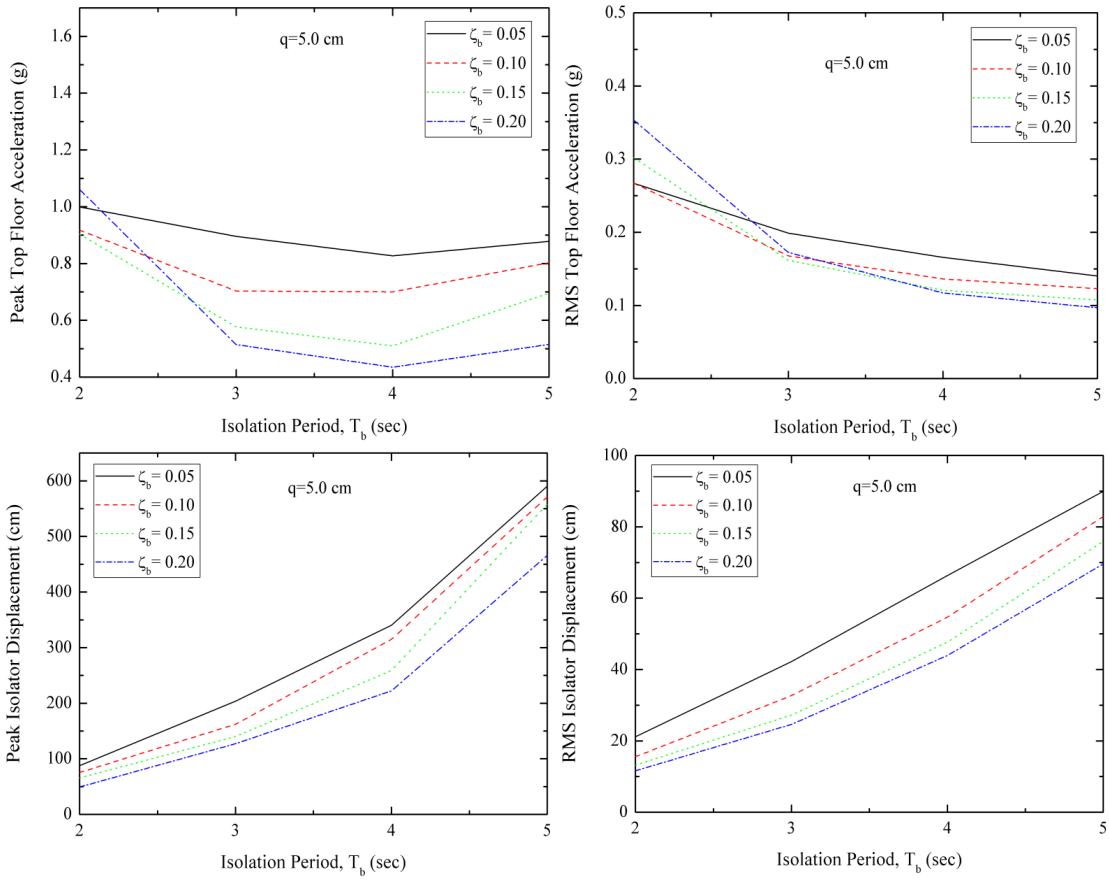

Figure 6.6: Variation of response quantities for different isolation periods, T_b and isolation damping ratios, ζ_b, $q = 5$ cm, 400 simulations

Chapter 7

Conclusion

7.1 Summary and Conclusion

In this study, a database of recorded earthquakes is created and a probabilistic method to generate artificial earthquakes based on recorded ground motions in the database is provided. Using Monte Carlo simulations, stochastic response of a five storey base-isolated building under earthquake excitations is reported by considering the earthquake parameters to be uncertain. A reliability analysis is done. A study on the parameters of the earthquake which produces very high responses is attempted. A parametric study based on the isolator characteristics is done.

Based on the work it is concluded that:

1. About 0.8 percent of the earthquakes simulated by using the probabilistic model produces very high responses. These earthquakes generally have very high average intensity in the strong motion phase.

2. The base isolation is very effective for more than 99 percent of the earthquakes generated.

3. The top floor acceleration decreases with the increase in the yield displacement of the isolator and the isolator displacement decreases with the increase in the yield displacement.

4. The isolation system with a long isolation period and high damping is the most effective.

7.2 Limitations

The probabilistic model developed is based on arbitrary recorded earthquakes. As a result, the earthquakes produced are highly random in nature. Therefore, studies using specific characteristics of earthquakes such as site conditions, fault type, etc cannot be studied.

The uncertainties in the characteristics of the structure and the isolator are neglected.

The accuracy of the Monte Carlo simulations depends largely on the number of simulation. Therefore, a large number of simulations are required which consumes a lot of time.

7.3 Future Scope of Work

An extensive database with earthquakes with specific characteristics like fault type, site characteristics etc can be developed. The model developed can be used to generate an earthquake of desired qualities.

The predictive equations used to predict the earthquake characteristics for a particular site can be combined with the ground motion model to produce a set of earthquakes pertaining to that site. By doing this, it will be possible to generate a ground motion for a particular site with an associated probability of occurrence of that particular ground motion. Software can be developed by using the database and the set of program developed which will be very useful for design engineers.

The uncertainties in the isolator characteristics and the structural characteristics like stiffness and damping can be modelled and a stochastic analysis of a base isolated structure under earthquake excitation can be done.

A comprehensive stochastic analysis of base isolated structure can be done by using non-sampling methods like the Karhunen Loeve method and the Polynomial Chaos method.

References

[1] www.seismicisolation.com/images accessed in march 2010.

[2] http://en.wikipedia.org/wiki/File:LRBtest.jpg accessed in march 2010.

[3] Papadimitriou K. Stochastic characterization of strong ground motion and application to structural response. Technical Report EERL 90-03, Accessed online at http://caltecheerl.library.caltech.edu/179/ in march 2010., California Institute of Technology, Pasadena, CA, 1990.

[4] Bulleit W.M. Uncertainty in structural engineering. *Practice Periodical on Structural Design and Construction*, 13:24–30, 2008.

[5] Pfeiffer F. and Wriggers P. *Uncertainty assessment of large finite element systems*. Springer-Verlag, Berlin, 2005.

[6] Kelly J.M. Aseismic base-isolation: review and bibliography. *Soil Dynamics and Earthquake Engineering*, 5:202–216, 1986.

[7] Buckle I.G. and Mayes R.L. Seismic isolation, history, application and performance- a world view. *Earthquake Spectra*, 6:161–201, 1990.

[8] Ibrahim R.A. Recent advances in non-linear passive vibration isolators. *Journal of Sound and Vibration*, 314:371–452, 2008.

[9] Jangid R.S. and Datta T.K. Seismic behavior of base-isolated building: a state-of-the-art-review. *Structures and Buildings*, 110:186–203, 1995.

[10] Matsagar V.A. and Jangid R.S. Influence of isolator characteristics on the response of base-isolated structures. *Engineering Structures*, 26:1735–1749, 2004.

[11] Sharma A. and Jangid R.S. Behaviour of base-isolated structures with high initial isolator stiffness. *International Journal of Applied Science, Engineering and Technology*, 5:199–204, 2009.

[12] Zerva A. Seismic source mechanisms and ground motion models, review paper. *Probabilistic Engineering Mechanics*, 3:64–74, 1988.

[13] Shinozuka M. and Deodatis G. Stochastic process models for earthquake ground motion. *Probabilistic Engineering Mechanics*, 3:114–123, 1988.

[14] Conte J.P. and Peng B.F. Fully nonstationary analytical earthquake ground-motion model. *Journal of Engineering Mechanics,ASCE*, 12:15–24, 1997.

[15] Kiureghian A.D. and Crempien J. An evolutionary model for earthquake ground motion. *Structural Safety*, 6:235–246, 1989.

[16] Rezaeian S. and Kiureghian A.D. A stochastic ground motion model with separable temporal and spectral nonstationarities. *Earthquake Engineering and Structural Dynamics*, 37:1565–1584, 2008.

[17] Schueller G.I. and Pradlwarter H.J. Uncertainty analysis of complex structural systems. *International journal for Numerical Methods in Engineering*, 80:881–913, 2009.

[18] Er G.K. and Iu V.P. Stochastic response of base-excited coulomb oscillator. *Journal of Sound and Vibration*, 233:81–92, 2000.

[19] Su L. and Ahmadi G. Response of frictional base isolation systems to horizontal-vertical random earthquake excitations. *Probabilistic Engineering Mechanics*, 3(1):12–21, 1988.

[20] Constantinou M.C. and Papageorgiou A.S. Stochastic response of practical sliding isolation systems. *Probabilistic Engineering Mechanics*, 5:27–34, 1990.

[21] Schueller G. I. Pradlwarter H. J. and Dorka U. Reliability of mdof-systems with hysteretic devices. *Engineering Structures*, 20(8):685–691, 1988.

[22] Yeh C.H. and Wen Y.K. Modeling of non-stationary ground motion and analysis of inelastic structural response. *Structural Safety*, 8:281–298, 1990.

[23] Alhan C. and Gavin H.P. Reliability of base isolation for the protection of critical equipment from earthquake hazards. *Engineering Structures*, 27:1435–1449, 2005.

[24] Naeim F. and Kelly J.M. *Design of isolated structures, from theory to practice.* John Wiley and Sons, New York, 1999.

[25] Chopra A.K. *Dynamics of structures: theory and applications to earthquake engineering.* Prentice-Hall, Englewood Cliffs, NJ, 2001.

[26] Wen Y.K. Method for random vibrations of hysteretic systems. *Journal of Engineering Mechanics division,ASCE*, 102:249–263, 1976.

[27] Housner G.W. and Jennings P.C. Generation of artificial earthquakes. *Journal of Engineering Mechanics division,ASCE*, 90:113–150, 1964.

[28] Wright M.H. Lagarias J.C., Reeds J.A. and Wright P.E. Convergence properties of the nelder-mead simplex method in low dimensions. *SIAM Journal of Optimization*, 9(1):112–147, 1998.

[29] Stuart A. and Ord J.K. *Kendall's advanced theory of statistics: distribution theory.* Halsted press, New York, 1994.

[30] Marburg S. Erstellung eines moduls zur analyse stochastischer signale fur das programmsystem sysken. Master's thesis, Technische Universitat Dresden, Germany, 1992.

[31] Papoulis A. *Probability, random variables and stochastic processes, third edition.* Mc Graw Hill, New York, 1991.

[32] Newland D.E. *An introduction to random vibrations, spectral and wavelet analysis.* Dover Publications, New York, 1993.

[33] Clough R.W. and Penzien J. *Dynamics of structures, third edition.* Computers and Structures, Inc., Berkeley, 2003.

[34] Ranganathan R. *Structural reliability analysis and design.* Jaico publishing house, New Delhi, 1999.

Vita

Mr. Cibi Jacob M has completed his masters degree in structural engineering from the Indian Institute of Technology (IIT) Delhi. He did his schooling at Zion Matriculation Higher Secondary School at Tambaram, Chennai. He obtained 96% aggregate in his school leaving examination in 2004. He secured the state rank for scoring centum in computer science subject. He got his bachelors degree in Civil Engineering from the College of Engineering Guindy, Anna University, Chennai. He scored 99.1 percentile in GATE 2008 examination. He was selected for the prestigious DAAD Sandwich Model Scholarship to work on his M. Tech. thesis project in Germany. He has provided structural consultancy services for a few buildings in Chennai and aspires to become a world renowned consultant. He is also a good cricketer.